NJC

New Journal of Chemistry

A journal for new directions in chemistry

Accepted Manuscript

This article can be cited before page numbers have been issued, to do this please use: T. C. Braga, T. F. Silva, T. M. S. Maciel, E. C. D. da Silva, E. F. da Silva-Júnior, L. V. Modolo, I. Figueiredo, J. Carinhanha, T. M. de Aquino and Â. de Fátima, *New J. Chem.*, 2019, DOI: 10.1039/C9NJ03556G.

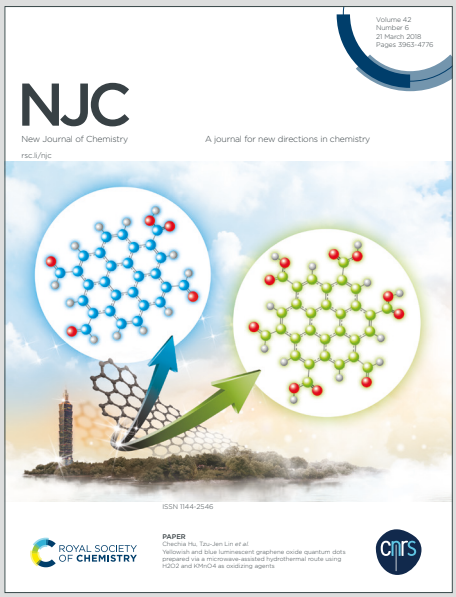

This is an Accepted Manuscript, which has been through the Royal Society of Chemistry peer review process and has been accepted for publication.

Accepted Manuscripts are published online shortly after acceptance, before technical editing, formatting and proof reading. Using this free service, authors can make their results available to the community, in citable form, before we publish the edited article. We will replace this Accepted Manuscript with the edited and formatted Advance Article as soon as it is available.

You can find more information about Accepted Manuscripts in the Information for Authors.

Please note that technical editing may introduce minor changes to the text and/or graphics, which may alter content. The journal's standard Terms & Conditions and the Ethical guidelines still apply. In no event shall the Royal Society of Chemistry be held responsible for any errors or omissions in this Accepted Manuscript or any consequences arising from the use of any information it contains.

View Article Online
DOI: 10.1039/C9NJ03556G

ARTICLE

Ionic Liquid-assisted Synthesis of Dihydropyrimidin(thi)ones Biginelli Adducts and Investigation of their Mechanism of Urease Inhibition

Received 00th January 20xx,
Accepted 00th January 20xx

DOI: 10.1039/x0xx00000x

Taniris Cafiero Braga,[a] Thamara Ferreira Silva,[b] Thamilla Maria Silva Maciel,[c] Edjan Carlos Dantas da Silva,[d] Edeildo Ferreira da Silva-Júnior,[d] Luzia Valentina Modolo,[b] Isis Martins Figueiredo,[c] Josué Carinhanha Caldas Santos,[c] Thiago Mendonça de Aquino,[d] Ângelo de Fátima,[a]*

Twenty-six Biginelli adducts were synthesized through an ionic liquid-assisted synthesis with up to 92% of yield. Sixteen of these Biginelli adducts were then assayed to determine their antiureolytic activity against purified urease from jack bean. The substances **BA7-S**, **BA9-S** and **BA11-S** showed to be as efficient inhibitors as hydroxyurea, a positive control used *in vitro* screening assay against urease. The fluorescent studies revealed that **BA7-S**, **BA9-S**, **BA11-S** and **BA5-S** possessed high binding constant values of $\log K_b$ = 5.95, 6.72, 4.55, 4.28 M^{-1}, respectively, while the **BAS12-S**, without substituents, showed low value of $\log K_b$ = 2.16 M^{-1}. In addition, in the most thermodynamically favorable **BA5-S** and **BA7-S** ureases complexes, the corresponding Biginelli adducts were capable of interact with the active sites of urease through non-ionic interactions, such as hydrophobic interactions, or hydrogen and Van der Walls interactions, respectively. *In silico* studies also supported that **BAs** display interaction in active site, confirming the fluorescence and for kinect studies which clear indicate that **BA5-S** and **BA7-S** are competitive inhibitors (K_i = 0.96 and 0.57 mM, respectively). *In silico* studies also showed that, the substituents in the aromatic ring are able to interact with Ni atoms to form a stable complex.

Introduction

In 1926, James B. Summer reported a historical accomplishment in biochemistry: the X-ray data for urease from jack beans - the first enzyme ever to be examined this way.[1,2] Since this pivotal finding, other ureases have been discovered and isolated from fungi, bacteria and other plants.[1,3] Depending on the source, altered subunits have been observed in different ureases. However, the structures of the active sites near the nickel (II) atoms are similar, and all ureases act by the same mechanism for the catalytic hydrolysis of urea. Due to these similarities, an inhibitor of one urease may also inhibit others.[4]

Urease catalyses urea hydrolysis, providing ammonium and carbamate 10^{14} times faster than the uncatalyzed reactions.[2,5] This enzyme is recognized as contributing to environmental problems, such as acid rain, since carbamate spontaneously provides CO_2 and ammonia.[3,5–7] In addition, several human pathogens, such as *Mycobacterium tuberculosis*, *Yersinia enterocolitica* and *Cryptococcus neoformans*, possess ureases as an essential virulence factor, leading to infections with urinary stones, pyelonephritis, ammonia encephalopathies, hepatic coma, and gastritis.[6,8–10] Moreover, approximately 100 megatons of nitrogen (N) fertilizer, which is one of the most used fertilizers worldwide, is mainly in the form of urea and leads to the urease-driven hydrolysis of urea on the soil surface yielding up to 70% N loss to the environment.[11,12]

Considering that the inhibition of ureases could control/mitigate many problems associated with ureases, such as human illness, agricultural production and environmental issues, several new urease inhibitors have been developed, and the understanding of how these new substances negatively affect ureases has been pursued.[4,13–18]

Urease inhibitors include different classes of substances such as flavonoids, quinolones, benzimidazoles, oxazoles, thiazolidines, organophosphorus compounds and dihydropyrimidinones/thiones (DHPMs, such as Biginelli adducts).[4,17–22] DHPMs are one of the most attractive substances for developing new urease inhibitors since they can be easily prepared through a multicomponent reaction (MCR). The first Biginelli adducts were described by Pietro Biginelli in 1891, in which different 1,3-dicarbonyl compounds were reacted with aldehydes and urea under the catalysis of HCl. [23] DHPMs, especially those derived from phenolic aldehydes (Figure), have shown good activities with IC_{50} values ranging

[a] Grupo de Estudos em Química Orgânica e Biológica (GEQOB), Departamento de Química, Universidade Federal de Minas Gerais, Belo Horizonte, MG, Brazil.
[b] Grupo de Estudos em Bioquímica de Plantas (GEBioPlan), Departamento de Botânica, Instituto de Ciências Biológicas, Universidade Federal de Minas Gerais, Belo Horizonte, MG, Brazil.
[c] Laboratório de Instrumentação e Desenvolvimento em Química Analítica (LINQA), Instituto de Química e Biotecnologia, Universidade Federal de Alagoas, Maceió, AL, Brazil.
[d] Núcleo de Análises e Pesquisa em Ressonância Magnética Nuclear (NAPRMN), Instituto de Química e Biotecnologia, Universidade Federal de Alagoas, Maceió, AL, Brazil.
*Corresponding author: Prof. Dr. Ângelo de Fátima: Tel.: +55-31-3409-6373. E-mail: adefatima@qui.ufmg.br

Electronic Supplementary Information (ESI) available: [details of any supplementary information available should be included here]. See DOI: 10.1039/x0xx00000x

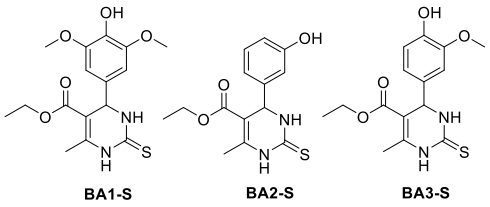

Figure 1. Chemical structures of dihydropyrimidinthiones [DHPMs; also known as Biginelli adducts (**BA**)] that possess urease inhibitor activity.

from 5.4 to 34.7 μM in different studies.[20,24,25] In addition to expressive antiureolytic activities of DHPMs, there have been few studies dedicated to elucidating the mechanism of action of ureases for this class of substances.[24,25]

Herein, we describe the synthesis of 26 Biginelli adducts, the *in vitro* screening for urease inhibitors of the synthesized substances, the systematic studies of enzyme/substrate interactions for these substances and the *in silico* studies for the most potent urease inhibitors.

Results and discussion

Synthesis of the Biginelli adducts

Biginelli adducts can be obtained under the catalysis of different Lewis or Brönsted acids, in the presence or absence of a protic or an aprotic solvent, under conventional or microwave heating.[25–28] Examples of Lewis acids that have been used include $InCl_3$, $SnCl_3$, $FeCl_3$ and $AlCl_3$,[29] and some examples of Brönsted acids include piperidine hydrochloride, sulfurous acid (H_2SO_3), hydrochloric acid (HCl) and *p*-toluenesulfonic acid (PTSA).[30] Among the Brönsted acid catalyst, ionic liquids (ILs) derived from imidazole have been recognized as efficient catalysts for Biginelli reactions.

ILs are salts in the liquid state, which have melting point values below an arbitrary temperature, such as 100 °C. ILs have a low vapor pressure, which in turn makes this class of substances interesting catalysts since their uses avoids the use of volatile solvents. In addition, these salts are generally miscible in the reaction media, and they are easily separated from the product, for instance, by adding water to the reaction mixture.[31] Based on these advantages of ILs, we prepared the ionic liquid [BIMBS][Cl] (**7**) (Figure) and used it as a catalyst to prepare a series of Biginelli adducts (**BAs**).The synthesis of the ionic liquid

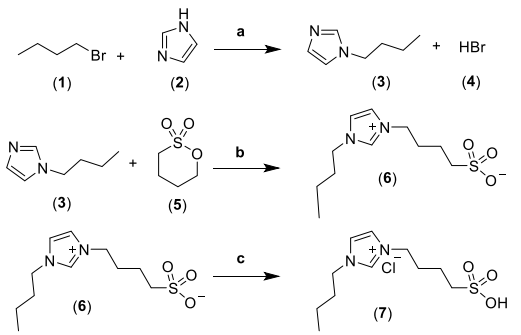

Figure 2. Synthetic route to ionic liquid [BIMBS][Cl] (7). Reagents and reaction conditions: (a) KOH, MeCN, reflux 4h, 69%; (b) 80°C, 24 h, 98%; (c) HCl reflux, 6 h, 100%.

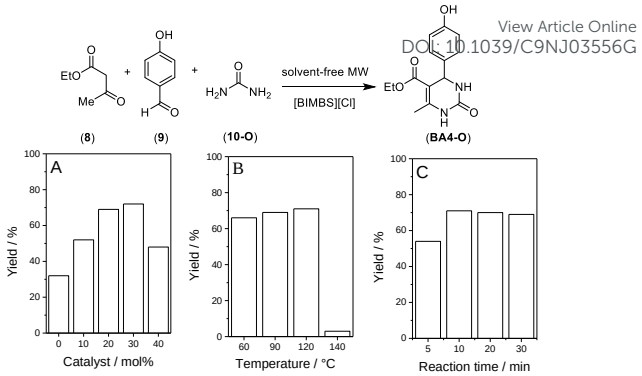

Figure 3. Effect of amount of ionic liquid [BIMBS][Cl] (**7**), temperature and time reaction for the preparation of Biginelli adduct derived from urea (**BA4-O**). Reagents and reaction conditions: 4-hydroxybenzaldehyde, ethyl acetoacetate and urea (1:1.5:1.5, respectively) under microwave irradiation [MW (power max 250 Watts)] in a DISCOVER CEM® reactor. (A) 90 °C, 30 min with different amount of **7**; (B) **7** (20 mol%), 30 min in different temperature; (C) **7** (20 mol%), 90°C for different reaction times.

[BIMBS][Cl] (**7**) started with the promotion of the substitution nucleophilic bimolecular reaction (S_N2) between *n*-bromobutane (**1**) and imidazole (**2**), in basic media, which furnished the 1-butyl-1*H*-imidazole (**3**) in 69% yield. Subsequently, **3** was treated with 1,4-butane sultone (**5**) to provide the zwitterionic substance **6** in 98% yield. Finally, treatment of **6** with HCl led to the ionic liquid [BIMBS][Cl] (**7**) in 68% overall yield (3 steps). The chemical characterization data for the ionic liquid **7** are in accordance with those published elsewhere. [32,33]

Having the ionic liquid **7** in hand, our efforts then focused on the use of this ionic liquid as a catalyst in the Biginelli reaction under microwave irradiation and solvent-free conditions. The Biginelli reaction of ethyl acetoacetate (**8**), 4-hydroxybenzaldehyde (**9**) and urea (**10-O**) (molar ratio of 1.5:1.0:1.5, respectively), under microwave irradiation (MW) and solvent-free conditions, was used as a model reaction (Figure). For the model reaction, it was determined that 20 mol% of **7**, at 90°C for 10 min under microwave irradiation were the best conditions to provide the compound **BA4-O** (71% yield) (Figure). Notably, only traces of the desirable products were formed when using conventional heating or room temperature.

After establishing the best reaction conditions for using **7** as the catalyst in the Biginelli reaction, we tested different aldehydes bearing electron-withdrawing and electron-donating substituents as well as one aliphatic aldehyde. Urea and thiourea were also used, and 26 Biginelli adducts were prepared; 13 **BA**s derived from urea (**BA1-O** to **BA13-O**) and 13 derived from thiourea (**BA1-S** to **BA13-S**) (Table 1). There was no clear evidence that the presence of electron-withdrawing and electron-donating substituents on the aromatic aldehydes positively or negatively influenced the yields values for the Biginelli reaction catalysed by **7**. However, the average yields for the aromatic aldehydes bearing electron-withdrawing substituents (58% for urea derivatives and 62% for thiourea derivatives) were slightly higher than those observed for the aromatic aldehydes bearing electron-donating substituents (55% for urea derivatives and 58% for thiourea derivatives) (Table 1).

Table 1. Scope of Biginelli reaction under the catalysis of ionic liquid [BIMBS][Cl] (**7**)[a].

BA	Structure	Yield (%)	BA	Structure	Yield (%)
BA1-O	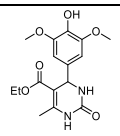	26	**BA1-S**	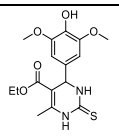	47
BA2-O	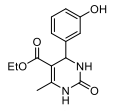	52	**BA2-S**	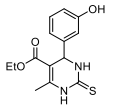	46
BA3-O	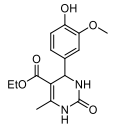	39	**BA3-S**	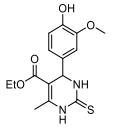	25
BA4-O	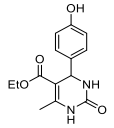	71	**BA4-S**	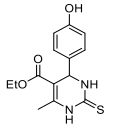	52
BA5-O	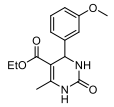	73	**BA5-S**	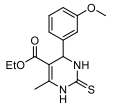	81
BA6-O	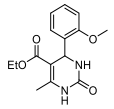	55	**BA6-S**	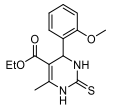	92
BA7-O	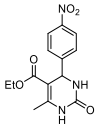	61	**BA7-S**	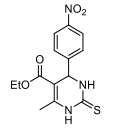	60
BA8-O	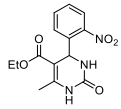	28	**BA8-S**	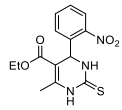	30
BA9-O	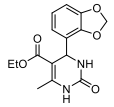	69	**BA9-S**	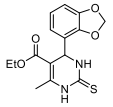	67
BA10-O	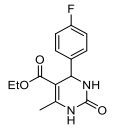	74	**BA10-S**	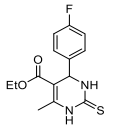	81
BA11-O	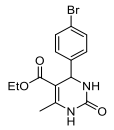	70	**BA11-S**	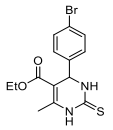	78
BA12-O	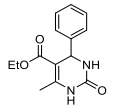	68	**BA12-S**	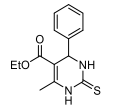	85
BA13-O	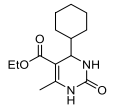	43	**BA13-S**	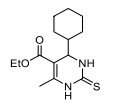	4

[a]Reagents and reaction conditions: Aldehyde, ethyl acetoacetate, urea or thiourea (1:1.5:1.5, respectively) and IL (20 mol%) under microwave irradiation [MW (power max 250 W, 90°C, holding time: 2 min and run time: 10 min)] in a DISCOVER CEM®.

Effects of Biginelli adducts on urease activity

The criteria for choosing the Biginelli adducts that would be tested for their potential to inhibition of *Canavalia ensiformis* (jack bean) urease relied on the selection of a representative group of compounds bearing electron donating or withdrawing substituents that were also soluble in ethanol.

The activity of jack bean urease is not affected by 10% ethanol, [26] while DMSO and other organic solvents that are required to dissolve substances with limited water solubility considerably inhibit the ureolytic activity of jack bean type III urease (data not shown).

The synthesized Biginelli adducts that contain a thiourea moiety were usually more soluble in ethanol than their corresponding urea derivatives. The *in vitro* screening revealed that the tested Biginelli adducts were classified into four categories according to their potential to inhibit urease (Figure ; Scott Knott test; $P < 0.05$). Therefore, the **BA7-S**, **BA9-S** and **BA11-S** were included in group A because they were as efficient as the reference inhibitor hydroxyurea (48.5% inhibition on average). **BA1-S**, **BA5-S**, **BA6-S** and **BA8-S** were placed into group B and effectively inhibited jack bean urease by 36% on average. Group C included **BA1-O**, **BA3-S**, **BA10-S** and **BA12-S** (average inhibition of 22.5%) while group D was constituted of compounds that poorly inhibited the enzyme (**BA2-O**, **BA9-O** – **BA12-O**; 14.3% inhibition on average). These results agree with those reported elsewhere, in which Biginelli adducts containing a thiourea core were much better urease inhibitors than those bearing urea core.[20,24] Additionally, the presence of electron donating or electron withdrawing substituents at the *para* position led to good antiureolytic activity of the Biginelli adducts.

Inhibitors **BA7-S**, **BA9-S** and **BA11-S** (from group A) were further used to study the interactions with jack bean urease. **BA5-S** and **BA12-S** were also chosen for this such study since the former is a representative of group B, while the latter is an example of a low potency urease inhibitor from a thiourea series that lacks a substituent on the phenyl ring (Table 1, Figure).

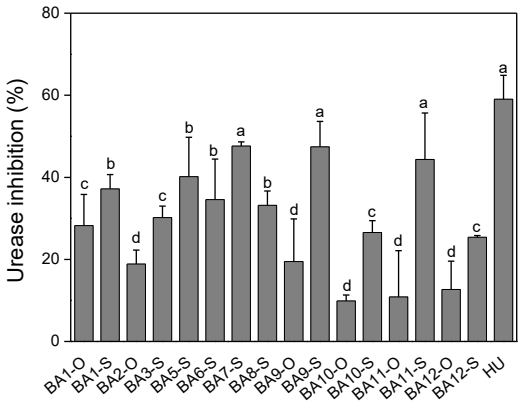

Figure 4. Effect of Biginelli adducts on the activity of jack bean urease. Buffered reactions contained 10 mM urea, 12.5 mU jack bean urease and 500 µM Biginelli adduct. Data are the means + standard deviation. Distinct letters indicate significant difference among the tested compounds (Scott Knott; $P < 0.05$). Hydroxiurea (HU) was used as reference of urease inhibitor.

Interaction between Biginelli adducts and jack bean urease investigated by molecular fluorescence

Interaction mechanism and thermodynamic parameters

The interaction studies between compounds **BA5-S**, **BA7-S**, **BA9-S**, **BA11-S** and, **BA12-S** and urease were carried out to understand the mechanism of enzyme inhibition exhibited by selected Biginelli adducts. Urease from *C. ensiformis* (jack bean) contains four Trp residues at positions 495, 648, 708, and 728; which at physiological pH are the main fluorophores (Φ = 0.20) in the enzyme, compared with Tyr (Φ = 0.14) and Phe (Φ = 0.04),[27] in native proteins, Tyr emission is often quenched, presumably by its interaction with the peptide chain or by energy transfer to Trp.[28] Therefore, urease intrinsic fluorescence is mainly a result of Trp residue contribution, which can them be used as a fluorophore for the studies of protein-ligand interactions and ligand-induced conformational changes around a binding site.[29]

The interaction process was evaluated using steady-state spectrofluorimetric titration based on the intrinsic urease fluorescence. The fluorescence spectra of urease in the absence and presence of increasing amounts of **BA7-S** are shown in Figure A. Similar profiles were obtained for other compounds. Upon excitation at 280 nm, urease presented a wide, intense band at 335 nm (Figure). After the addition of **BA7-S** to the system, there was a decrease in the fluorescence intensity and variation of the maximum emission wavelength from 335 to 345 nm. The signal intensity reduction and the redshift of the maximum wavelength was attributed to conformational changes in the structure of the enzyme.[30] To evaluate the interaction strength between urease and the Biginelli adduct selected, the binding constant (K_b) was calculated:

$$\log\left[\frac{(F_0 - F)}{F}\right] = \log K_b + n\log[Q] \qquad \text{equation (1)}$$

where F_0 and F are the respective fluorescence intensities in the absence and presence of the ligand, K_b is the binding constant and *n* is the number of binding sites in the enzyme.[31] Figure B shows the respective linearization of equation 1 to calculate the binding parameters related to K_b and *n,* using the compounds **BA5-S** and **BA7-S**.

To evaluate the affinity of the selected Biginelli adducts against urease, the respective binding constant values were compared. Based on Figure C, compounds **BA5-S** and **BA7-S** show the highest K_b values, hence, these compounds were employed as models for the mechanistic enzyme inhibition studies. The results of this study are presented in Table 2 for the temperatures 23, 30, and 37 °C. In addition, **BA20-S** presented the lowest enzyme affinity, corroborating the results of the urease inhibition experiments (Figure).

The binding constant (K_b) expresses the strength of the interaction between a ligand and a protein and for the Biginelli adducts, it was found that the interaction between **BA7-S** and urease was stronger than that of **BA5-S** and urease (Table 2). The K_b values for these Biginelli adducts toward the enzyme were in the same range as those reported for the interaction between jack bean urease and (*R*)-(+)-usnic acid (3.55×10^6 M^{-1} at 30°C) [32] and Cu(II) (3.89×10^5 M^{-1} at 37°C when [Cu(II)] < 16 µM) [33], and higher than pentachlorophenol (3.85×10^3 M^{-1} at 32°C) [27] and Cr(VI) (1.96×10^4 M^{-1} at 29°C). However, the authors of these studies did not evaluate the potential of pentachlorophenol, Cr(VI) ($K_2Cr_2O_7$) and Cu(II) as urease inhibitors. According to equation 1, *n* corresponds to the number of occupied sites by the ligand in the urease structure. The values of *n* varied from 1.07 to 1.38, indicating that the interactions among these ligands and urease occurred at a ratio of 1:1.

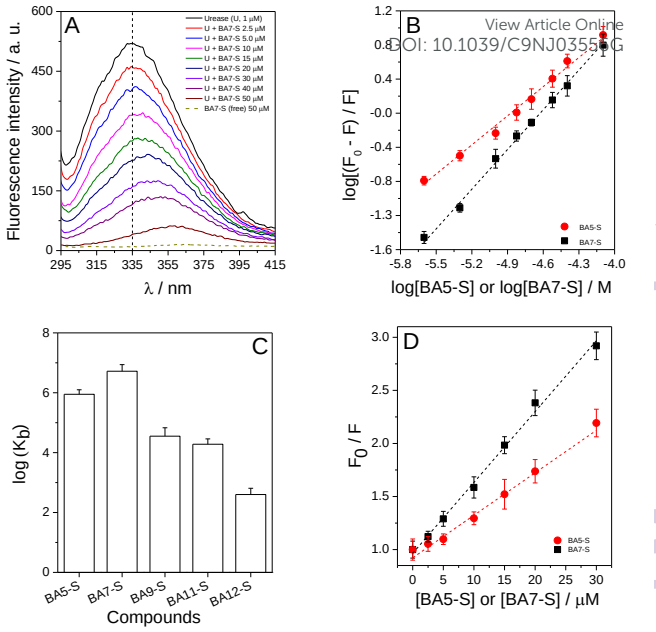

Figure 5. Interactions between jack bean urease and BA5-S or BA7-S. Values (B – D) are the means (n = 3) ± standard deviation. (A) Emission spectral profile of urease (1.0 µM) in the presence of 2.5 – 50 µM BA7-S at pH 7 and 30 °C; (B) Double logarithmic curve to determine the binding constant (Kb) for BA5-S and BA7-S; (C) Binding constants of all tested Biginelli adducts in relation to jack bean urease; (D) Stern-Volmer quenching plot for BA5-S and BA7-S as a function of BAs concentration.

To evaluate the interaction mechanism between urease and the Biginelli adducts, the Stern-Volmer equation was applied:

$$\frac{F_0}{F} = 1 + K_q\tau_0[Q] = 1 + K_{SV}[Q] \qquad \text{equation (2)}$$

where K_q is the diffusional bimolecular velocity quenching constant, τ_0 is the average life time (10^{-8} s), [Q] is the concentration of the ligand (quencher), and K_{SV} is the Stern-Volmer quenching constant.[34] Due to the elevation of the diffusion coefficient and a greater number of collisions between the fluorophores (protein) and the quenchers, a dynamic quenching process would be observed if the K_{SV} values increases with temperature. An opposing profile was observed in the static quenching process, since at higher temperatures, the stability of the protein-ligand complex is affected. According to these results (Table 2), the values of the quenching constant (K_{SV}) decreased with increasing temperature for both ligands. Thus, the interaction process between **BA5-S** and **BA7-S** and urease occurred preferentially through a static quenching mechanism with the formation of a supramolecular enzyme-ligand complex.[35] Additionally, all K_q values were calculated to

View Article Online
DOI: 10.1039/C9NJ02556G

be greater than 2.0×10^{12} M^{-1} s^{-1} , confirming that static quenching occurred.[36]

The binding of small molecules to proteins usually occurs through noncovalent interactions, thus, the thermodynamic parameters were obtained using the linearized Van't Hoff equation (equation 3) from interaction assays performed at different temperatures. These parameters permit the deduction of the kind of forces involved in the enzyme-inhibitor interaction (Table 2). The Gibbs free energy (ΔG) was calculated according to equation 4.

Table 2. Binding and thermodynamics parameters for urease interaction with Biginelli's adduct **BA5-S** and **BA7-S**.

Compound	T (°C)	Stern-Volmer constant			Binding constant parameters			Thermodynamic parameters		
		K_{SV} (10^4 M^{-1})	r	K_q (10^{12} M^{-1} s^{-1})	K_b (10^6 M^{-1})	*n*	r	ΔG (kJ mol^{-1})	ΔH (kJ mol^{-1})	ΔS (J mol^{-1} K^{-1})
BA5-S	22	4.96 ± 0.14	0.9872	4.96	0.66 ± 0.03	1.36 ± 0.04	0.9862	-32.88		
	30	4.70 ± 0.10	0.9853	4.70	0.91 ± 0.10	1.22 ± 0.05	0.9944	-34.54	+28.37	+207.6
	38	4.46 ± 0.06	0.9887	4.46	1.20 ± 0.15	1.07 ±0.03	0.9873	-36.20		
BA7-S	22	9.11 ± 0.26	0.9861	9.11	8.49 ± 0.46	1.29 ± 0.02	0.9971	-39.14		
	30	8.99 ± 0.15	0.9779	8.99	5.27 ± 0.52	1.23 ± 0.06	0.9873	-38.98	-45.19	-20.50
	38	8.30 ± 0.09	0.9891	8.30	3.29 ± 0.37	1.38 ± 0.02	0.9962	-38.91		

$$\log K_b = -\frac{\Delta H}{R}\times\left[\frac{1}{T}\right] + \frac{\Delta S}{R} \qquad \text{equation (3)}$$

$$\Delta G = \Delta H - T\Delta S \qquad \text{equation (4)}$$

where T is the temperature in Kelvin (K) and R is the ideal gas constant. Figure S1 (Supporting Information) shows a graphical representation of the linearized Van't Hoff equation.

Considering the negative values of ΔG obtained (Table 2) the evaluated interaction process was thermodynamically spontaneous. The main relationship between the forces involved in the interaction process, and the enthalpy and entropy variation values are as follows: $\Delta H > 0$ and $\Delta S > 0$ (hydrophobic forces); $\Delta H < 0$ and $\Delta S > 0$ (electrostatic forces), and $\Delta H < 0$ and $\Delta S < 0$ (hydrogen bonds and Van der Waals forces). [37] The predominant binding forces (nonexclusive) for Biginelli adduct **BA5-S** were hydrophobic interactions, and for **BA7-S** the predominant forces were hydrogen bonds and Van der Waals forces.

Förster resonance energy transfer (FRET)

FRET studies were employed to determine the distance between the urease tryptophan residues (donor) and Biginelli adducts (receptors) in the process of energy transfer due to interaction. The distance (r_0) between the donor and the receptor can be calculated using equation 5:

$$E = 1 - \frac{F}{F_0} = \frac{R_0^6}{R_0^6 + r_0^6} \qquad \text{equation (5)}$$

where F_0 and F are the fluorescence intensity of the donor in the absence and presence of the ligand; respectively, E is the fraction of energy transferred from the donor to the receptor, and R_0 is the critical distance (when 50% of the donor's emission energy is transferred to the receiver). This critical distance (R_0) is mathematically described as:

$$R_0^6 = 8.79\times10^{-25} K^2 N^{-4} \Phi J \qquad \text{equation (6)}$$

where K^2 is the dipole orientation of the donor and the receptor, *N* is the mean refractive index, Φ is the quantum yield of the protein fluorescence, and *J* represents the overlapping area of the donor's normalized emission spectrum in relation to the receptor absorption spectrum. In this case, $K^2 = 2/3$, $N = 1.336$ and $\Phi = 1.50$ for urease.[33] The overlap area (*J*) can be calculated by the equation:

$$J = \frac{\int_0^\infty F(\lambda)\varepsilon(\lambda)\lambda^4 d\lambda}{\int_0^\infty F(\lambda) d\lambda} \qquad \text{equation (7)}$$

In this equation, F(λ) is the fluorescence of the donor and ε(λ) is the molar absorption coefficient of the receptor, which can be obtained through Beer's law.[38] Initially, the overlap area between the fluorescence spectra of free urease and the molecular absorption spectra of **BA5-S** and **BA7-S** were evaluated (Fig. S2, Supporting Information). The calculated parameters for the FRET process are shown in Table 3.

Table 3. FRET parameters for urease interaction with Biginelli adducts **BA5-S** and **BA7-S**. Enzyme and Biginelli adducts at 5 μM.

Compound	*J* (10^{-15} cm^3 M^{-1})	E (%)	R_0 (nm)	r_0 (nm)
BA5-S	4.0	34	2.16	2.42
BA7-S	7.5	44	2.40	2.50

According to the results (Table 3), the energy transferred (E) was less than 50%, implying that $R_0 < r_0$; and the values of the distances of r_0 for **BA5-7** and **BA7-S** are similar. The critical distances r_0 between the Biginelli adducts and Trp residues (in urease) were less than 8 nm, indicating that the energy transfer

View Article Online
DOI: 10.1039/C9NJ03556G

ARTICLE

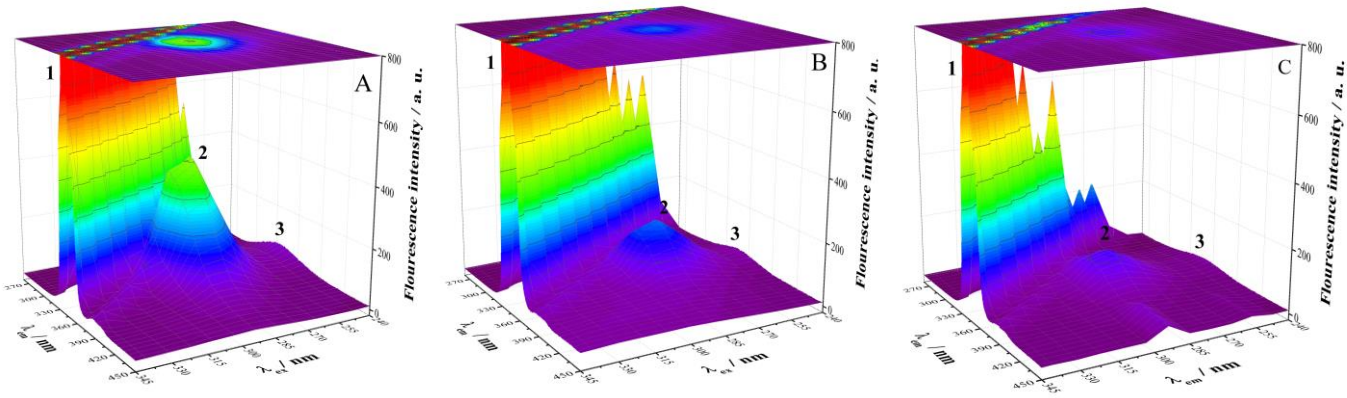

Figure 6. Tridimensional fluorescence spectra of urease (A), **BA5-S**-urease complex (B) e **BA7-S**-urease complex (C) at pH 7. Enzyme and ligands were used at 1.0 and 40 µM, respectively.

occurred after the interaction process [39]. Once the evaluated compounds interacted effectively with the urease, we assessed whether the interaction process led to changes in the conformation of the enzyme.

Evaluation of the conformational changes of urease

The three-dimensional fluorescence spectrum allows more detailed information about the typical conformational changes in the secondary structure of a protein to be obtained [40]. The three-dimensional fluorescence spectra for urease by itself or complexed with **BA5-S** and **BA7-S** are presented in Figure . The three-dimensional fluorescence spectra of free urease and complexed urease show peak 1, which corresponds to Rayleigh scattering, which is characterized by irradiation re-emission ($\lambda_{ex} = \lambda_{em}$) from water (solvent). Peak 2 corresponds to the emission of the Trp and Tyr residues while the emission of the polypeptide backbone in the urease structure is represented by peak 3.[31,40] The fluorescence intensities of peaks 2 and 3 were reduced by 53 and 60%, respectively, after the addition of **BA5-S** (Table S1, Supporting Information). A similar spectral profile was recorded for the systems containing **BA7-S**; a 72 and 79% reduction in the fluorescence intensity was observed for peaks 2 and 3, respectively. The main parameters of tridimensional fluorescence are listed in Table S1.

The reduction in fluorescence intensity corresponding to peak 2 indicated changes in theTrp and Tyr microenvironment, while alterations related to peak 3 indicated modifications to the native protein structure. The most significant variations in fluorescence intensity were observed for peak 3, indicating that alterations in the polypeptide chain and enzyme folding.[41] In addition, these results are supported by the variation of the Stokes shift determined for native urease and the respective inhibitor-enzyme complexes (Table S1).

Synchronous fluorescence studies were performed to observe the preferential interactions and changes in the urease fluorophore (Tyr and Trp) microenvironment. Differences between the excitation and emission wavelengths were used as parameters to evaluate polarity changes in the amino acid residues, since a $\Delta\lambda$ = 15 nm (Figure S3A and C, Supporting Information) provides information about the Tyr residue, while a $\Delta\lambda$ = 60 nm (Figure S3B and D, Supporting Information) shows changes in the Trp residue.[42] The synchronous fluorescence binding parameters for **BA5-S** and **BA7-S** towards urease are shown in Table 4.

The maximum wavelength emission shifts for Biginelli adducts **BA5-S** and **BA7-S** towards urease were higher for Trp than for Tyr (Table 4). This is based on the fact that Tyr residues are less sensitive to medium polarity changes when compared to Trp. An increase in the microenvironment polarity is related to a positive variation in λ_{max}, while polarity reduction is associated with a negative variation in λ_{max}. These phenomena allow us to describe changes in the structure of native proteins

Table 4. Synchronous fluorescence binding parameters for Biginelli's adducts **BA5-S** and **BA7-S** towards urease.

Compound	$\Delta\lambda$ (nm)	Stern-Volmer parameters		λ_{max} emission shift (nm)[1]
		K_{SV} (10^4 M^{-1})	r	
BA5-S	15	4.24 ± 0.08	0.9691	-1
	60	2.91 ± 0.04	0.9880	+6
BA7-S	15	10.21 ± 0.12	0.9656	+1
	60	6.49 ± 0.09	0.9705	+4

[1]Free urease was used as reference. The error represents the SD for the three determinations.

to the presence of Tyr at positions 410 and 544 near the key His residues (positions 409 and 545) responsible for coordinating to Ni atoms in the jack bean urease active site.[43] Considering that the Trp residues (495 and 648) are far away from the urease catalytic site, the Tyr residues had their microenvironment changed more significantly than Trp.[32] Therefore, the Biginelli adducts **BA5-S** and **BA7-S** interact with the urease catalytic site.

Competition assay

The effect of some classical inhibitors [*N*-butyl thiophosphoric triamide (NBPT), thiourea, hydroxyurea and omeprazole] on the interaction of urease with Biginelli adducts **BA5-S** and **BA7-S** was evaluated by competition assay. The urease binding constant ratio (K_b'/K_b), in which K_b' and K_b refer to as the binding constant in the presence or absence of a competitor, respectively, was used for comparison purposes. The formation of urease-ligand complexes is favored when $K_b'/K_b > 1$ while ratios lower than 1 indicate that complex formation is disfavored (Table 5).

Table 5. Urease binding constants ratio in the absence (K_b) or presence (K_b') of urease inhibitors.

Compound	Competitors (K_b'/K_b)[a]			
	NBPT	Omeprazole	Thiourea	Hydroxyurea
BA5-S	0.32 ± 0.08	0.40 ± 0.10	0.66 ± 0.07	0.31 ± 0.03
BA7-S	0.46 ± 0.02	0.53 ± 0.03	0.53 ± 0.02	0.33 ± 0.02[b]

[a]K_b' = binding constant in the presence of inhibitor (25 μM), urease (1 μM) varying Biginelli adducts (2.5 - 50 μM). [b]Hydroxyurea inhibitor was used at 38 μM. The error represents the SD for the three determinations.

In general, the binding constant decreases in the presence of inhibitors ($K_b'/K_b < 1$), indicating that Biginelli adducts **BA5-S** and **BA7-S** interact with the urease active site. This result is in agreement with the results of the synchronous fluorescence assays (Table 4). Thiourea, hydroxyurea and NBPT are competitive inhibitors,[44] while omeprazole is classified as a noncompetitive inhibitor by reacting with the free Cys592 residue of jack bean urease, which causes blockage of the access of urea to the enzyme catalytic site.[45] Additionally, the affinity of **BA5-S** and **BA7-S** to the urease catalytic site was confirmed by UV-vis spectroscopic tests, which showed interaction between these Biginelli adducts and Ni(II) ions in solution (Figure S4). Finally, the results presented herein show that **BA5-S** and **BA7-S** interact with the urease active site, however, competition assays are limited to differentiate between competitive and mixed inhibitors. Thus, to unequivocally assess the type of inhibitor, we applied a classic enzymatic kinetics assay.

Kinetics assay

BA5-S, which possesses an electron donor substituent at the *meta* position, and **BA7-S**, which bears an electron withdrawing group at the *para* position, were chosen to determine the mechanism by which they inhibit urease activity. Both compounds were found to be typical competitive inhibitors because the urease V_{max} was not affected by the presence of increasing concentrations of **BA5-S** or **BA7-S** (**Error! Reference source not found.**). Additionally, the $K_{M\ app}$ for urea increased with increasing of urease inhibitor concentrations in the reaction medium. Moreover, both **BA5-S** and **BA7-S** can compete with urea for the active site of jack bean urease to form urease-**BA5-S** and urease-**BA7-S** complexes, respectively. The Lineweaver-Burk plots (Figure - C and D) allowed for the calculation of the equilibrium dissociation constants for such complexes (K_i). The K_i value for the urease-**BA5-S** complex was determined to be 0.96 ± 0.01 mM while this same value for the urease-**BA7-S** complex was 0.57 ± 0.16 mM. These results indicate that the Biginelli adduct **BA7-S** is a more potent inhibitor of jack bean urease than **BA5-S**. Because the inhibitor affinity for the enzyme is inversely proportional to K_i, the kinetics results are in accordance with those obtained from the molecular fluorescence experiments (Table 2).

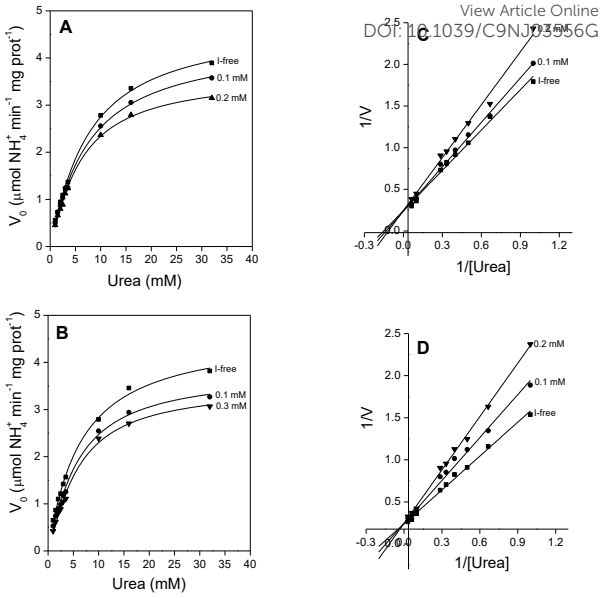

Figure 7. Representative Michaelis–Menten hyperbola (A and B) and Lineweaver-Burk (C and D) plots for jack bean urease in the presence of **BA5-S** (A and C) or **BA7-S** (B and D). Increasing concentrations of urea (1-32 mM) were incubated for 10 min with jack bean type III urease in the absence (I-free) or presence of inhibitor (0.1 to 0.3 mM). I-free, free of urease inhibitor.

Molecular Dynamics and Docking simulation

For structural validation and stereochemical quality of the jack bean urease, the refined model was confirmed by Ramachandran plot analysis. It revealed that 89.2% of the amino acid residues are located in the most favored region, 9.1% are located in the allowed region, and only 1.7% is located in the outlier region (Figure **Error! Reference source not found.**). Additionally, the RMSD graphic was generated for C_α atoms, showing that the system reaches the equilibrium phase after 20 ns (Fig. S5, Supporting Information). Thus, the generated model of jack bean urease was geometric and stereochemically acceptable and the stabilized structure was used as the starting point for molecular docking studies.

For the docking protocol validation, a self-docking experiment was performed, where the co-crystallized acetohydroxamic acid (HAE) was removed from the ligand-binding domain of the jack bean urease, and then a flexibly re-docked was performed. The

View Article Online
DOI: 10.1039/C9NJ03556C

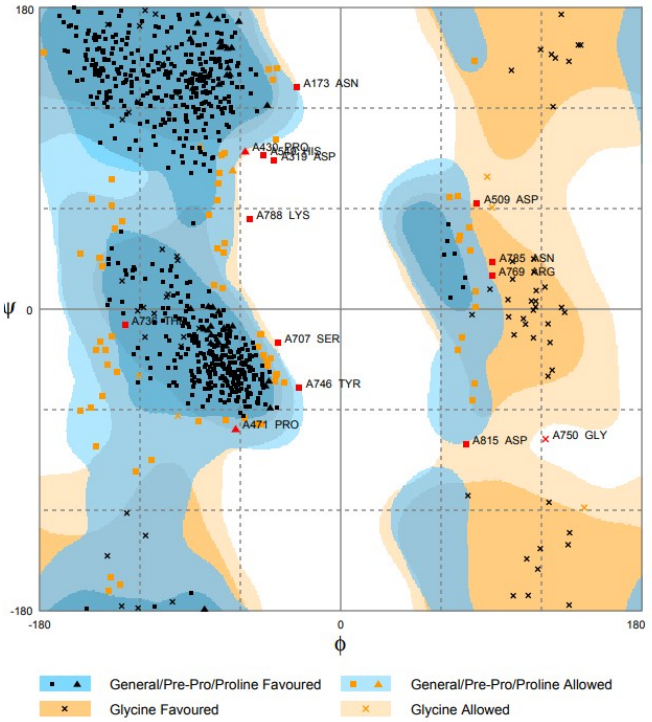

Figure 8. Ramachandran plot showing the distribution of the Phi (φ) and Psi (ψ) dihedral angles of the proline and glycine amino acids in the jack bean urease.

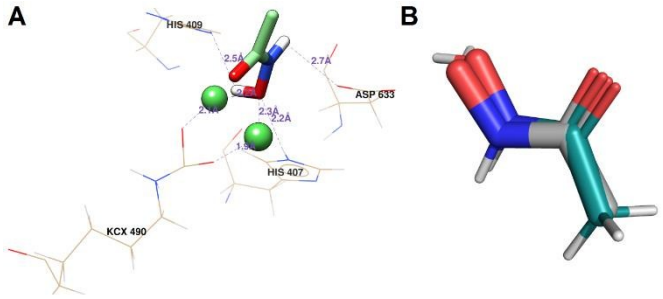

Figure 9. (A) Re-docking pose of HAE in the active site of the jack bean urease, showing the same interactions when compared with the co-crystallized ligand. (B) Superposition of co-crystallized and re-docked HAE conformations. The two Ni metals are represented as green spheres. Coordination with Ni metals and hydrogen bonding are shown as dotted lines.

re-docked HAE-enzyme complex revealed the same ligand's coordination with two nickel ions *via* hydroxyl oxygen, when compared with the crystallographic complex (Figure A). RMSD value obtained by comparison between the crystallized and re-docked ligand was computed as 0.737 Å, suggesting that this virtual protocol is effective for the analysis of binding modes of the Biginelli adducts. In Figure B, it is shown the superposition of co-crystallized and re-docked HAE.

The docking study performed with the active compounds **BA5-S** and **BA7-S** revealed a similarity in the fitting-in mechanism at the same active site when compared with HAE. For both compounds, was observed that the orientation of aryl ring plays an important role in the stable complexes formation, due to the methoxy (Figure A) or nitro coordination (Figure B) with the bi-nickel center of the enzyme. In addition, in both **BA5-S** and **BA7-S** complexes, Ni ions are chelated with carbamylated Lysine KCX490 residue.

The analysis of the predicted binding conformation of the most active compound **BA7-S** showed that further stability was due to the formation of hydrogen bonding interactions between His[492], Gly[550], and Arg[609] with carbonyl or thiocarbonyl groups. In addition, the aryl ring is involved in *π*-*π* stacking and anion-*π* interaction with His[519] and Asp[633], respectively (**Error! Reference source not found.**B). Binding modes of compound **BA5-S** is shown in Figure 3A, where hydrogen bonding

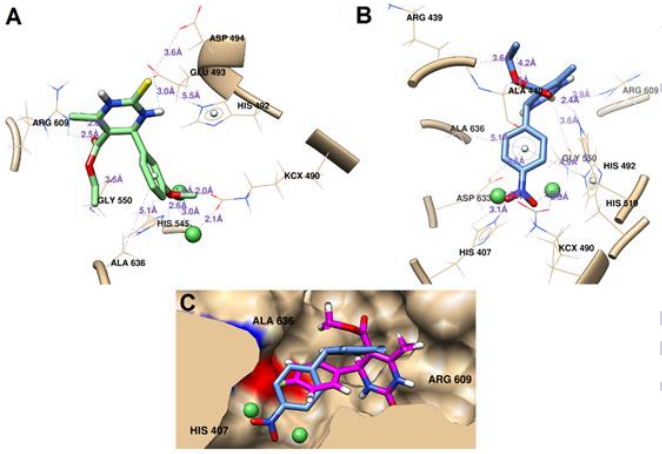

Figure 10. Interactions of **BA5-S** (A) and **BA7-S** (B) with Ni metals and residues of jack bean urease. C - Comparison between the docked conformations of the most active compound **BA7-S** and weak urease inhibitor **BA10-S** in the catalytic cavity of the enzyme. Compound **BA7-S** (blue). Compound **BA10-S** (pink). The binding conformation of the Biginelli adducts are shown in stick representation and the two Ni metals are represented by green spheres. Coordination with Ni metals, hydrogen bonding, π-π stacking, anion-π, and sulfur-π interactions are shown with dotted lines.

interactions were observed between carbonyl and NH groups with Arg[605] and Glu[492] residues, respectively. Additional sulfur-*π* interactions were observed between the thiourea group and His[492] and Asp[494] residues. In general, **BA5-S** and **BA7-S** derivatives display interactions in the catalytic site similarly to the others active Biginelli adducts described in the literature [20,46]. In addition, an *in silico* study carried out with a less active thiourea derivative bearing *p*-F at the phenyl ring (**BA10-S**) revealed that such Biginelli adduct also anchors to the urease catalytic cavity. However, the lack of coordination with Ni metals prevents the formation of a stable ligand-enzyme complex, which appears to be responsible for its lower inhibitory activity on urease (**Error! Reference source not found.**C) [20] Finally, the theoretical studies were in agreement with the experimental data.

Conclusions

Twenty-six **BA**s were successfully synthesized (yields of up to 92%) by using [BIMBS][Cl] as catalyst. **BA7-S**, **BA9-S** and **BA11-S** were as effective as hydroxyurea to inhibit urease activity. *In silico* tests suggest that the aromatic substituents in the **BA** structures form complexes with the nickel atoms present in the urease active site. Sulfur-*π* interactions between the thiourea group and the residues His[492] and Asp[494] of urease contribute to the potency of such urease inhibitors. All these theoretical studies are supported by fluorescence (competition, 3D and synchronous) and the kinetic assays that revealed high binding constants (> 4) towards the jack bean urease active site for **BA5-**

S and **BA7-S** with mechanisms of action typical of competitive inhibitors. The *in silico* studies suggest that slight modifications on the aromatic rings of the **BA**s can modulate their ability to inhibit urease.

General experimental procedures

The reagents used were provided by commercial sources and were of analytical grade. For reaction monitoring, thin-layer chromatography (TLC) Polygram-UV2540, mm MACHEREY-NAGEL (20 x 20 cm) was used. Chromatographic purification was performed using 100-200 mesh silica gel. The melting point was recorded by Gehaka-PF1500 apparatus, and the observed values were not corrected. All infrared spectra were acquired using a Spectro One Perkin Elmer or Bruker model Alpha spectrometer at 400-4000 cm^{-1}. Samples were prepared using KBr plate or ATR method. NMR was recorded with a Bruker AVANCE DPX 200 or 400 spectrometer with a BBO multinuclear probe.

Synthesis and characterization

Synthesis of the ionic liquid [BIMBS][Cl] (7)

1-Butyl-1*H*-imidazole (**3**): *n*-Bromobutane (2.4 mmol) (**1**), imidazole (3.0 mmol) (**2**) and KOH (6.0 mmol) were added to acetonitrile (5.0 mL). The reaction mixture was stirred and refluxed for 4 h. After this period, the reaction mixture was dissolved in dichloromethane (20 mL) and extracted with distilled water (3×20 mL). The organic layer was collected and dried over magnesium sulphate, and the solvent was removed using rotatory evaporation. The obtained crude reaction product was then purified using silica gel column chromatography, and a mixture of ethyl acetate:hexane:dichloromethane (6:1:1) was used as the eluent. 1-Butyl-1*H*-imidazole (3) was obtained as a yellow liquid in 69% yield. IR (ATR, ν cm^{-1}): 3111, 2960, 1667. ^{1}H-NMR (200 MHz, $CDCl_3$) δ 0.86 (3H, t , *J* = 7.3 Hz), 1.24 (2H, sex, *J* = 7.3 Hz), 1.69 (2H, quin, *J* = 7.2 Hz), 3.86 (2H, t, *J* = 7.2 Hz), 6.83 (1H, s), 6.97 (1H, s), 7.43 (1H, s). ^{13}C-NMR (50 MHz, $CDCl_3$) δ 13.4 ($\underline{C}H_3$), 19.7 ($\underline{C}H_2$), 33.0 ($\underline{C}H_2$), 46.8 ($\underline{C}H_2$), 188.8 ($\underline{C}H$), 128.9 ($\underline{C}H$), 136.9 ($\underline{C}H$). HRMS (ESI): *m/z* observed: 125.1026; $C_7H_{12}N_2$ $[M+H]^+$ calculated: 125.1079; error (ppm): 4.2. All data for 3 are in accordance with those reported elsewhere. [47]

4-(1-Butyl-1*H*-imidazol-3-ium-3-yl)butane-1-sulfonate (**6**): 1-Butyl-1*H*-imidazole (**3**) (1.12 mmol) and 1,4-butane sultone (1.21 mmol) (**5**) were added to toluene (0.5 mL). The reaction mixture was stirred at 80°C for 24 h. Subsequently, the reaction mixture was cooled down to room temperature, and ethyl ether was slowly added with magnetic stirring until a white solid precipitated. The solid material was filtrated and dried under vacuum, providing **6** in 78% yield. IR (ATR, ν cm^{-1}): 3125, 2962, 1648, 1175. M.p. = 76.8-79.3 °C (Lit. M.p. = 136°C) [56]. ^{1}H-NMR (200 MHz, DMSO-d_6) δ 0.86 (3H, t, *J* = 7.3 Hz), 1.24 (2H, sex, *J* = 7.3 Hz), 1.53 (2H, quin, *J* = 7.0 Hz), 1.69-1.92 (4H, m), 2.42-2.46 (2H, m), 4.13-4.22 (4H, m), 7.82 (2H, brs), 9.28 (1H, brs). ^{13}C-NMR (50 MHz, DMSO-d_6) δ 13.3 ($\underline{C}H_3$), 18.8 ($\underline{C}H_2$), 21.8 ($\underline{C}H_2$), 28.6 ($\underline{C}H_2$), 31.2 ($\underline{C}H_2$), 48.5 ($\underline{C}H_2$, $\underline{C}H_2$), 50.4 ($\underline{C}H_2$), 122.4 ($\underline{C}H$, $\underline{C}H$), 136.1 ($\underline{C}H$). All data for **6** are in accordance with those reported elsewhere.[48]

1-Butyl-3-(4-sulfobutyl)-1*H*-imidazol-3-ium chloride {[BIMBS][Cl]} (**7**): 4-(1-Butyl-1*H*-imidazol-3-ium-3-yl)butane-1-sulfonate (**6**) (3.8 mmol) was dissolved in an aqueous solution of HCl (37%, 3.8 mmol). The solution was stirred under reflux for 6 h, and then the water was evaporated under vacuum. 1-Butyl-3-(4-sulfobutyl)-1*H*-imidazol-3-ium chloride (**7**) was obtained as a viscous liquid in 100% yield. IR (ATR, ν cm^{-1}): 3144, 2963, 1647, 1162. ^{1}H-NMR (200 MHz, DMSO-d_6) δ 0.88 (3H, t, *J* = 7.4 Hz), 1.24 (2H, sex, *J* = 7.4 Hz), 1.54 (quin, 2H, *J* = 7.5 Hz), 1.69-1.96 (4H, m), 2.54 - 2.57 (2H, m), 4.14 - 4.23 (4H, m), 7.83 (2H, s), 9.34 (1H, s). ^{13}C-NMR (50 MHz, DMSO-d_6) δ 13.3 ($\underline{C}H_3$), 18.7 ($\underline{C}H_2$), 21.6 ($\underline{C}H_2$), 28.6 ($\underline{C}H_2$) 31.2 ($\underline{C}H_2$), 48.6 ($\underline{C}H_2$), 50.5 ($\underline{C}H_2$), 122.5 ($\underline{C}H$, $\underline{C}H$), 136.1 ($\underline{C}H$).

General procedure for the synthesis of Biginelli adducts with the catalyst [BIMBS][Cl] (7)

A mixture of ethyl acetoacetate (**8**) (1.5 mmol), an aldehyde (1 mmol), urea (**10-O**) (1.5 mmol) or thiourea (**10-S**) (1.5 mmol) and **7** (0.2 mmol – 20 mol%) was heated under microwave irradiation (MW) in a DISCOVER CEM® reactor (conditions: 90°C, 200-250 W, 10 min). Subsequently, the reaction mixture was dissolved in hot ethanol (~50°C), and then water was added until the solution appeared muddy. The mixture was magnetically stirred for 10 min, and the solid obtained was filtered and dried under vacuum. Some Biginelli adducts required purification by silica gel column chromatography.

Ethyl 4-(4-hydroxy-3,5-dimethoxyphenyl)-6-methyl-2-oxo-1,2,3,4-tetrahydropyrimidine-5-carboxylate (**BA1-O**): 26% yield (purified by precipitation). IR (KBr, ν cm^{-1}): 3614, 3232, 3102, 2952, 1726, 1708, 1654, 1120. M.p. = 182.3-183.4 °C. ^{1}H-NMR (200 MHz, DMSO-d_6) δ 1.12 (t, 3H, *J* = 6.5 Hz), 2.24 (s, 3H), 3.70 (s, 6H), 4.01 (q, 2H, *J* = 6.5 Hz), 5.08 (s, 1H), 6.48 (s, 2H), 7.65 (s, 1H), 8.32 (s, 1H), 9.13 (s, 1H). ^{13}C-NMR (50 MHz, DMSO-d_6) δ 14.2 ($\underline{C}H_3$), 17.7 ($\underline{C}H_3$), 53.8 ($\underline{C}H$), 56.0 ($\underline{C}H_3$), 59.1 ($\underline{C}H_2$), 99.4 ($\underline{C}$), 103.9 ($\underline{C}H$), 135.0 ($\underline{C}$), 147.8 ($\underline{C}$), 152.2 ($\underline{C}$), 165.5 ($\underline{C}$). All data for **BA1-O** are in accordance with those reported elsewhere.[49]

Ethyl 4-(4-hydroxy-3,5-dimethoxyphenyl)-6-methyl-2-thioxo-1,2,3,4-tetrahydropyrimidine-5-carboxylate (**BA1-S**): 47% yield (purified by precipitation). IR (KBr, ν cm^{-1}): 3476, 3330, 3198, 2946, 1668, 1648, 1186, 1112. M.p.: 2013.0-214.3°C. ^{1}H-NMR (200 MHz, DMSO-d_6) δ 1.13 (t, 3H, *J* = 7.0 Hz), 2.28 (s, 3H), 3.71 (s, 6H), 4.04 (4, 2H, *J* = 7.0 Hz), 5.11 (d, 1H, *J* = 2.9 Hz), 6.46 (s, 2H), 8.42 (s, 1H), 9.58 (s, 1H), 10.29 (s, 1H). ^{13}C-NMR (50 MHz, DMSO-d_6) δ 14.1 ($\underline{C}H_3$), 17.1 ($\underline{C}H_3$), 53.8 ($\underline{C}H$), 56.0 ($\underline{C}H_3$), 59.6 ($\underline{C}H_2$), 101.0 ($\underline{C}$), 104.0 ($\underline{C}H$), 133.7 ($\underline{C}$), 135.4 ($\underline{C}$), 144.7 ($\underline{C}$), 147.9 ($\underline{C}$), 165.3 ($\underline{C}$), 174.3 ($\underline{C}$). All data for **BA1-S** are in accordance with those reported elsewhere.[49]

Ethyl 4-(3-hydroxyphenyl)-6-methyl-2-oxo-1,2,3,4-tetrahydropyrimidine-5-carboxylate (**BA2-O**): 52% yield (purified by precipitation). IR (KBr, ν cm^{-1}): 3514, 3354, 3246,

2980, 1726, 1700, 1602, 1192. M.p.: 183.7-185.0 °C (Lit. M.p.: 190-192 °C).[50] ^{1}H-NMR (400 MHz, DMSO-d_6) δ 1.11 (t, 3H, J = 7.0 Hz), 2.23 (s, 3H), 3.99 (q, 2H, J = 7.0 Hz), 5.06 (d, 1H, J = 2.7 Hz), 6.62 (d, 1H, J = 7.9 Hz), 6.66-6.67 (m, 2H), 7.08 (t, 1H, J = 7.9 Hz), 7.69 (s, 1H), 9.16 (s, 1H), 9.36 (s, 1H). ^{13}C-NMR (100 MHz, DMSO-d_6) δ 14.1 (CH$_3$), 17.8 (CH$_3$), 53.9 (CH), 59.2 (CH$_2$), 99.4 (C), 113.1 (CH), 114.2 (CH), 116.9 (CH), 129.3 (CH), 146.3 (C), 148.1 (C), 152.3 (C), 157.4 (C), 165.4 (C). All data for **BA2-O** are in accordance with those reported elsewhere.[50]

Ethyl 4-(3-hydroxyphenyl)-6-methyl-2-thioxo-1,2,3,4-tetrahydropyrimidine-5-carboxylate (**BA2-S**): 46% yield (purified by precipitation), IR (KBr, ν cm^{-1}): 3308, 3184, 3116, 2984, 1684, 1662, 1196. M.p.: 183.4-185.1 °C (Lit. M.p.: 185-187 °C).[51] ^{1}H-NMR (200 MHz, DMSO-d_6) δ 1.11 (t, 3H, J = 7.1 Hz), 2.28 (s, 3H), 4.05 (q, 2H, J = 7.1 Hz), 5.01 (d, 1H, J = 3.6 Hz), 6.63- 6.67 (m, 3H), 7.12 (t, 1H, J = 8.1 Hz), 9.45 (s, 1H), 9.60 (brs, 1H), 10.30 (s, 1H). ^{13}C-NMR (50 MHz, DMSO-d_6) δ 14.1 (CH$_3$), 17.2 (CH$_3$), 54.0 (CH), 59.6 (CH$_2$), 100.8 (C), 113.3 (CH), 114.7 (CH), 117.0 (CH), 129.5 (CH), 144.9 (C), 157.5 (C), 165.2 (C), 174.2 (C). All data for **BA2-S** are in accordance with those reported elsewhere.[51]

Ethyl 4-(4-hydroxy-3-methoxyphenyl)-6-methyl-2-oxo-1,2,3,4-tetrahydropyrimidine-5-carboxylate (**BA3-O**): 39% yield (purified by precipitation), IR (KBr, ν cm^{-1}): 3538, 3244, 3116, 2974, 1704, 1698, 1644, 1170. M.p.: 233.9-236.0 °C (Lit. M.p.: 226 - 228 °C).[52] ^{1}H-NMR (200 MHz, DMSO-d_6) δ 1.11 (t, 3H, J = 7.1 Hz), 2.24 (s, 3H), 3.72 (s, 3H), 3.99 (q, 2H, J = 7.1 Hz), 5.06 (d, 1H, J = 2.9 Hz), 6.58–6.73 (m, 2H), 6.78-6.80 (m, 1H), 7.65 (s, 1H), 8.92 (s, 1H), 9.13 (s, 1H). ^{13}C-NMR (50 MHz, DMSO-d_6) δ 14.2 (CH$_3$), 17.8 (CH$_3$), 53.6 (CH), 55.6 (CH$_3$), 59.2 (CH$_2$), 99.6 (C), 110.9 (CH), 115.3 (CH), 118.3 (CH), 136.0 (C), 145.8 (C), 147.3 (C), 148.0 (C), 152.3 (C), 165.5 (C). All data for **BA3-O** are in accordance with those reported elsewhere.[52]

Ethyl 4-(4-hydroxy-3-methoxyphenyl)-6-methyl-2-thioxo-1,2,3,4-tetrahydropyrimidine-5-carboxylate (**BA3-S**): 25% yield (purified by precipitation), IR (KBr, ν cm^{-1}): 3418, 3160, 3000, 2952, 1682, 1652, 1196, 1112. M.p.: 224.9-225.5 °C (Lit. M.p.: 206-208 °C).[52] ^{1}H-NMR (200 MHz, DMSO-d_6) δ 1.11 (t, 3H, J = 7.0 Hz), 2.28 (s, 3H), 3.72 (s, 3H), 4.02 (q, 2H, J = 7.0 Hz), 5.09 (d, 1H, J = 2.8 Hz), 6.57-6.60 (m, 1H), 6.71-6.78 (m, 2H), 9.02 (s, 1H), 9.57 (s, 1H), 10.27 (s, 1H). ^{13}C-NMR (50 MHz, DMSO-d_6) δ 14.1 (CH$_3$), 17.2 (CH$_3$), 53.7 (CH$_3$), 55.6 (CH), 59.6 (CH$_2$), 101.0 (C), 111.0 (CH), 115.4 (CH), 118.6 (CH), 134.6 (C), 144.7 (C), 146.2 (C), 147.4 (C), 165.3 (C), 174.1 (C). All data for **BA3-S** are in accordance with those reported elsewhere.[52]

Ethyl 4-(4-hydroxyphenyl)-6-methyl-2-oxo-1,2,3,4-tetrahydropyrimidine-5-carboxylate (**BA4-O**): 71% yield (purified by precipitation). IR (KBr, ν cm^{-1}): 3504, 3270, 3113, 2982, 1678, 1640, 1600, 1088. M.p.: 231.9-234.8 °C (Lit. M.p.: 237-239 °C).[53] ^{1}H-NMR (200 MHz, DMSO-d_6) δ 1.09 (t, 3H, J = 6.9 Hz), 2.23 (s, 3H), 3.97 (q, 2H, J = 6.9 Hz), 5.04 (s, 1H), 6.68 (d, 2H, J = 8.0 Hz), 7.03 (d, 2H, J = 8.0 Hz), 7.62 (s, 1H), 9.12 (s, 1H), 9.34 (s, 1H). ^{13}C-NMR (50 MHz, DMSO-d_6) δ 14.5 (CH$_3$), 18.1 (CH$_3$), 53.8 (CH), 59.5 (CH$_2$), 100.1 (C), 115.4 (CH), 127.8 (CH), 135.8 (C), 148.1 (C), 152.6 (C), 156.9 (C), 165.8 (C). All data for **BA4-O** are in accordance with those reported elsewhere.[53]

Ethyl 4-(4-hydroxyphenyl)-6-methyl-2-thioxo-1,2,3,4-tetrahydropyrimidine-5-carboxylate (**BA4-S**): 52% yield (purified by precipitation). IR (KBr, ν cm^{-1}): 3422, 3286, 3198, 3022, 1716, 1662, 1198, 1084. M.p.: 202.7-205.7 °C (Lit. M.p.: 212-215 °C).[54] ^{1}H-NMR (200 MHz, DMSO-d_6) δ 1.09 (t, 3H, J = 7.1 Hz), 2.27 (s, 3H), 3.99 (q, 2H, J = 7.1 Hz), 5.06 (d, 1H, J = 3.4 Hz), 6.70 (d, 2H, J = 8.4 Hz), 7.00 (d, 2H, J = 8.4 Hz), 9.42 (s, 1H), 9.55 (s, 1H), 10.24 (s, 1H). ^{13}C-NMR (50 MHz, DMSO-d_6) δ 14.1 (CH$_3$), 17.1 (CH$_3$), 53.6 (CH), 59.5 (CH$_2$), 101.1 (C), 115.1 (CH), 127.7 (CH), 134.1 (C), 144.1 (C), 156.9 (C), 165.2 (C), 173.9 (C). All data for (**BA4-S**) are in accordance with those reported elsewhere.[54]

Ethyl 4-(3-methoxyphenyl)-6-methyl-2-oxo-1,2,3,4-tetrahydropyrimidine-5-carboxylate (**BA5-O**): 73% yield (purified by precipitation). IR (KBr, ν cm^{-1}): 3242, 3104, 2934, 1702, 1648, 1600, 1164. M.p.: 221.3-223.9 °C (Lit. M.p.: 219-220°C). [52] ^{1}H-NMR (200 MHz, DMSO-d_6) δ 1.11 (t, 3H, J = 7.1 Hz), 2.24 (s, 3H), 3.72 (s, 3H), 3.99 (q, 2H, J = 7.1 Hz), 5.12 (d, 1H, J = 2.9 Hz), 6.78-6.83 (m, 3H), 7.24 (t, J = 3.8, 1H), 7.74 (brs, 1H), 9.20 (s, 1H). ^{13}C-NMR (50 MHz, DMSO-d_6) δ 14.1 (CH$_3$), 17.8 (CH$_3$), 53.8 (CH), 55.0 (CH$_3$), 59.3 (CH$_2$), 99.2 (C), 112.2 (CH), 112.4 (CH), 118.3 (CH), 129.6 (CH), 146.4 (C), 148.5 (C), 152.3 (C), 159.2 (C), 165.4 (C). All data for **BA5-O** are in accordance with those reported elsewhere.[52]

Ethyl 4-(3-methoxyphenyl)-6-methyl-2-thioxo-1,2,3,4-tetrahydropyrimidine-5-carboxylate (**BA5-S**): 81% yield (purified by precipitation). IR (KBr, ν cm^{-1}): 3320, 3176, 2992, 1668, 1652, 1192, 1098. M.p.: 160.9-162.8 °C (Lit. M.p.: 141-143 °C).[52] ^{1}H-NMR (200 MHz, DMSO-d_6) δ 1.11 (t, 3H, J = 7.0 Hz), 2.28 (s, 3H), 4.02 (q, 2H, J = 7.0 Hz), 5.15 (d, 1H, J = 3.0 Hz), 6.72 (d, 1H, J = 2.0 Hz), 6.79 (d, 1H, J = 7.8 Hz), 6.84 (dd, 1H, J_3 = 7.8 Hz, J_4 = 2.0 Hz), 7.26 (t, 1H, J = 7.8 Hz), 9.65 (s, 1H), 10.35 (s, 1H). ^{13}C-NMR (50 MHz, DMSO-d_6) δ 14.0 (CH$_3$), 17.2 (CH$_3$), 53.8 (CH), 55.0 (CH$_3$), 59.7 (CH$_2$), 100.6 (C), 112.5 (CH), 112.5 (CH), 118.4 (CH), 129.8 (CH), 145.0 (C), 145.1 (C), 159.3 (C), 165.2 (C), 174.4 (C). All data for **BA5-S** are in accordance with those reported elsewhere.[52]

Ethyl 4-(2-methoxyphenyl)-6-methyl-2-oxo-1,2,3,4-tetrahydropyrimidine-5-carboxylate (**BA6-O**): 55% yield (purified by precipitation). IR (KBr, ν cm^{-1}): 3256, 3108, 2958, 1726, 1702, 1636, 1080. M.p.: 261.0-262.6 °C (Lit. M.p: 260-262 °C).[55] ^{1}H-NMR (200 MHz, DMSO-d_6) δ 1.02 (t, 3H, J = 7.0 Hz), 2.27 (s, 3H), 3.79 (s, 3H), 3.91 (q, 2H, J = 7.0 Hz), 5.49 (brs, 1H), 6.83-7.03 (m, 3H), 7.19-7.27 (m, 2H), 9.12 (s, 1H). ^{13}C-NMR (100 MHz, DMSO-d_6) δ 14.0 (CH$_3$), 17.7 (CH$_3$), 48.9 (CH), 55.4 (CH$_3$), 59.0 (CH$_2$), 97.6 (C), 111.1 (CH), 120.2 (CH), 127.1 (CH), 128.7 (CH),131.6 (C), 148.9 (C), 152.2 (C), 156.5 (C), 165.4 (C). All data for **BA6-O** are in accordance with those reported elsewhere.[55]

Ethyl 4-(2-methoxyphenyl)-6-methyl-2-thioxo-1,2,3,4-tetrahydropyrimidine-5-carboxylate (**BA6-S**): 92% yield

View Article Online
DOI: 10.1039/C9NJ03756G

(purified by precipitation). IR (KBr, ν cm^{-1}): 3260, 3270, 2998, 1710, 1652, 1178. M.p.: 185.5-187.9 °C (Lit. M.p.: 230-231 °C).[56] ^{1}H-NMR (400 MHz, DMSO-d_6) δ 1.37 (t, 3H, J = 7.1 Hz), 2.29 (s, 3H), 3.37 (s, 3H), 3.94 (qd, 2H, J_3 = 7.1 Hz, J_4 = 1.5 Hz), 5.50 (d, 1H, J = 3.4 Hz), 6.89 (td, 1H, J_3 = 7.6 Hz, J_4 = 0.7 Hz), 7.00 (d, 1H, J = 8.1 Hz), 7.04 (dd, 1H, J_3 = 7.6 Hz, J_4 = 1.6 Hz), 7.25 (td, 1H, J_3 = 7.6 Hz, J_4 = 1.6 Hz), 9.24 (d, 1H, J = 1.6 Hz), 10.23 (s, 1H). ^{13}C-NMR (100 MHz, DMSO-d_6) δ 13.9 (CH$_3$), 17.1 (CH$_3$), 49.5 (CH), 55.5 (CH$_3$), 59.4 (CH$_2$), 99.4 (C), 111.3 (CH), 120.2 (CH), 127.8 (CH), 129.2 (CH), 130.6 (C), 145.2 (C),156.6 (C), 165.2 (C), 174.2 (C). All data for **BA6-S** are in accordance with those reported elsewhere.[56]

Ethyl 6-methyl-4-(4-nitrophenyl)-2-oxo-1,2,3,4-tetrahydropyrimidine-5-carboxylate (**BA7-O**): 61% yield (purified by precipitation). IR (KBr, ν cm^{-1}): 3238, 3122, 2988, 1782, 1700, 1646, 1522, 1096, 856. M.p.: 201.9-206.7 °C (Lit. M.p.: 211-212 °C).[50] ^{1}H-NMR (200 MHz, DMSO-d_6) δ 1.09 (t, 3H, J = 7.1 Hz), 2.27 (s, 3H), 3.98 (q, 2H, J = 7.1 Hz), 5.28 (d, 1H, J = 3.1 Hz), 7.51 (d, 2H, J = 8.7 Hz), 7.90 (s, 1H), 8.22 (d, 2H, J = 8.7 Hz), 9.37 (s, 1H). ^{13}C-NMR (50 MHz, DMSO-d_6) δ 14.1 (CH$_3$), 17.9 (CH$_3$), 53.7 (CH), 59.4 (CH$_2$), 98.2 (C), 123.8 (CH), 127.7 (CH), 146.7 (C), 149.4 (C), 151.8 (C), 152.0 (C), 165.1 (C). All data for **BA7-O** are in accordance with those reported elsewhere.[50]

Ethyl 6-methyl-4-(4-nitrophenyl)-2-thioxo-1,2,3,4-tetrahydropyrimidine-5-carboxylate (**BA7-S**): 60% yield (purified by precipitation), IR (KBr, ν cm^{-1}): 3298, 3170, 2988, 1682, 1652, 1520, 1352, 1174, 853. M.p.: 193,0-195,6 °C (Lit. M.p.: 193-194 °C).[56] ^{1}H-NMR (200 MHz, DMSO-d_6) δ 1.09 (t, 3H, J = 7.0 Hz), 2.31 (s, 3H), 4.00 (q, 2H, J = 7.0 Hz), 5.39 (d, 1H, J = 3,1 Hz), 7.48 (d, 2H, J = 8.4 Hz), 8.23 (d, 2H, J = 8.4 Hz), 9.77 (s, 1H), 10.50 (s, 1H). ^{13}C-NMR (50 MHz, DMSO-d_6) δ 14.0 (CH$_3$), 17.3 (CH$_3$), 53.7 (CH), 59.8 (CH$_2$), 99.7 (C), 124.0 (CH), 127.8 (CH), 146.0 (C), 146.9 (C), 150.4 (C) 164.9 (C), 174.5 (C). All data for **BA7-S** are in accordance with those reported elsewhere.[56]

Ethyl 6-methyl-4-(2-nitrophenyl)-2-oxo-1,2,3,4-tetrahydropyrimidine-5-carboxylate (**BA8-O**): 28% yield [purified by silica gel column chromatography using ethyl acetate/hexane (3:1) as the eluant]. IR (KBr, ν cm^{-1}): 3366, 3222, 2988, 1698, 1646, 1608, 1524, 1370, 1094, 860. M.p.: 220.5-222.5 °C (Lit. M.p.: 205-206 °C).[55] ^{1}H-NMR (400 MHz, DMSO-d_6) δ 0.92 (t, 3H, J = 7.1 Hz), 2.28 (s, 3H), 3.82-3.85 (m, 2H), 7.51-7.57 (m, 2H), 7.71-7.73 (m, 2H), 7.88-7.90 (m, 1H), 9.36 (s, 1H). ^{13}C-NMR (100 MHz, DMSO-d_6) δ 13.7 (CH$_3$), 17.7 (CH$_3$), 49.4 (CH), 59.1 (CH$_2$), 96.0 (C), 123.9 (CH), 128.7 (CH), 129.0 (CH), 134.1 (CH), 139.3 (C), 147.5 (C), 149.6 (C), 151.2 (C), 164.7 (C). All data for **BA8-O** are in accordance with those reported elsewhere.[55]

Ethyl 6-methyl-4-(2-nitrophenyl)-2-thioxo-1,2,3,4-tetrahydropyrimidine-5-carboxylate (**BA8-S**): 30% yield [purified by silica gel column chromatography using ethyl acetate/hexane (3:1) as the eluant]. IR (KBr, ν cm^{-1}): 3292, 3190, 2982, 2982, 1722, 1657, 1524, 1354, 1196, 1094, 860. M.p.: 204.5-205.1 °C (Lit. M.p.: 195-197 °C).[56] ^{1}H-NMR (400 MHz, DMSO-d_6) δ 0.94 (t, 3H, J = 7.1 Hz), 2.31 (s, 3H), 3.81-3.93 (m, 2H), 5.95 (d, 1H, J = 2.8 Hz), 7.50-7.57 (m, 2H), 7.93 (td, 1H, J_3 = 8.2 Hz, J_4 = 1.1 Hz), 7.76 (dd, 1H, J_3 = 7.6 Hz, J_4 = 1.1 Hz), 9.56 (s, 1H), 10.44 (s, 1H). ^{13}C-NMR (100 MHz, DMSO-d_6) δ 13.7 (CH$_3$), 17.1 (CH$_3$), 49.2 (CH), 59.5 (CH$_2$), 99.8 (C), 124.2 (CH), 129.1 (CH), 129.4 (CH), 134.2 (CH), 136.0 (C), 145.6 (C), 147.3 (C), 164.5 (C), 174.1 (C). All data for **BA8-S** are in accordance with those reported elsewhere.[56]

Ethyl 4-(benzo[*d*][1,3]dioxol-4-yl)-6-methyl-2-oxo-1,2,3,4-tetrahydropyrimidine-5-carboxylate (**BA9-O**): 69% yield (purified by precipitation). IR (KBr, ν cm^{-1}): 3222, 3106, 2966, 1702, 1690, 1640, 1094. M.p.: 186.9-189.4 °C. ^{1}H-NMR (200 MHz, DMSO-d_6) δ 1.10 (t, 3H, J = 7.0 Hz), 2.24 (s, 3H), 3.99 (q, 2H, J = 7.0 Hz), 5.07 (brs, 1H), 5.97 (s, 2H), 6.67- 6.68 (m, 3H), 7.68 (s, 1H), 9.18 (s, 1H). ^{13}C-NMR (50 MHz, DMSO-d_6) δ 14.1 (CH$_3$), 17.8 (CH$_3$), 53.7 (CH), 59.2 (CH$_2$) 99.3 (C), 101.0 (CH$_2$), 106.7 (CH), 108.0 (CH), 119.3 (CH), 138.9 (C), 146.3 (C), 147.2 (C), 148.2 (C), 152.1 (C), 165.3 (C). All data for **BA9-O** are in accordance with those reported elsewhere.[49]

Ethyl 4-(benzo[*d*][1,3]dioxol-4-yl)-6-methyl-2-thioxo-1,2,3,4-tetrahydropyrimidine-5-carboxylate (**BA9-S**): 67% yield (purified by precipitation). IR (KBr, ν cm^{-1}): 3316, 3180, 2980, 1654, 1576, 1192, 1112. M.p.: 172,6-174,3 °C. ^{1}H-NMR (200 MHz, DMSO-d_6) δ 1.10 (t, 3H, J = 7.1 Hz), 2.29 (s, 3H), 4.01 (q, 2H, J = 7.1 Hz), 5.09 (d, 1H, J = 3.5 Hz), 5.99 (s, 2H), 6.66-6.71 (m, 2H), 6.87 (d, 1H, J = 6.9 Hz), 9.59 (s, 1H), 10,31 (s, 1H). ^{13}C-NMR (50 MHz, DMSO-d_6) δ 14.1 (CH$_3$), 17.2 (CH$_3$), 53.7 (CH), 59.6 (CH$_2$), 100.8 (C), 101.1 (CH), 106.7 (CH$_2$), 108.2 (CH), 119.7 (CH), 137.5 (C), 145.0 (C), 146.7 (C), 147.4 (C), 165.1 (C), 174.1 (C). Data for **BA9-S** are in accordance with those reported elsewhere.[49]

Ethyl 4-(4-fluorophenyl)-6-methyl-2-oxo-1,2,3,4-tetrahydropyrimidine-5-carboxylate (**BA10-O**): 74% yield (purified by precipitation). IR (KBr, ν cm^{-1}): 3246, 3124, 2980, 1728, 1714,1648, 1220, 1100. M.p.: 179.5-180.7 °C (Lit. M.p.: 172-173 °C).[52] ^{1}H-NMR (200 MHz, DMSO-d_6) δ 1.08 (t, 3H, J = 7.1 Hz), 2.25 (s, 3H), 3.98 (q, 2H, J = 7.1 Hz), 5.14 (d, 1H, J = 3.2 Hz), 7.14 (t, 2H, J = 7.3 Hz), 7.24-7.28 (m, 2H), 7.73 (s, 1H), 9.21 (s, 1H), ^{13}C-NMR (50 MHz, DMSO-d_6) δ 14.1 (CH$_3$), 17.8 (CH$_3$), 53.4 (CH), 59.2 (CH$_2$), 99.1 (C), 115.1 (CH), 126.2 (CH), 141.1 (C), 148.5 (C), 151.9 (C), 160.1 (C), 162.5 (C), 165.3 (C). All data for **BA10-O** are in accordance with those reported elsewhere.[52]

Ethyl 4-(4-fluorophenyl)-6-methyl-2-thioxo-1,2,3,4-tetrahydropyrimidine-5-carboxylate (**BA10-S**): 81% yield (purified by precipitation). IR (KBr, ν cm^{-1}): 3328, 3274, 2986, 1682, 1682, 1656, 1284, 1196, 1118. M.p.: 190.3-192.0 °C (Lit. M.p.: 194-195 °C).[57] ^{1}H-NMR (400 MHz, DMSO-d_6) δ 1.09 (t, 3H, J = 7.1 Hz), 2.30 (s, 3H), 4.00 (qd, 2H, J_3 = 7.1 Hz, J_4 = 3.4 Hz), 5.18 (d, 1H, J = 3.4), 7.15-7.20 (m, 2H), 7.23-7.26 (m, 2H), 9.64 (brs, 1H), 10.35 (s,1H). ^{13}C-NMR (100 MHz, DMSO-d_6) δ 14.0 (CH$_3$), 17.2 (CH$_3$), 53.4 (CH), 59.6 (CH$_2$), 100.6 (C), 115.3 (CH), 128.4 (CH), 139.7 (C), 145.1 (C), 160.3 (C),162.7 (C), 165.0 (C), 174.2

(C). All data for **BA10-S** are in accordance with those reported elsewhere.[57]

Ethyl 4-(4-bromophenyl)-6-methyl-2-oxo-1,2,3,4-tetrahydropyrimidine-5-carboxylate (**BA11-O**): 70% yield (purified by precipitation). IR (KBr, ν cm^{-1}): 3244, 3116, 2980, 1722, 1704, 1650, 1088, 678. M.p.: 212.3-215.3 °C (Lit. M.p.: 225-226 °C).[50] ^{1}H-NMR (200 MHz, DMSO-d_6) δ 1.09 (t, 3H, J = 6.9 Hz), 2.25 (s, 3H), 3.98 (q, 2H, J = 6.9 Hz), 5.13 (s, 1H), 7.52 (d, 2H, J = 8.2 Hz), 7.19 (d, 2H, J = 8.2 Hz), 7.77 (s, 1H), 9.25 (s, 1H), ^{13}C-NMR (50 MHz, DMSO-d_6) δ 14.4 ($\underline{C}H_3$), 18.2 ($\underline{C}H_3$), 53.9 ($\underline{C}H_2$), 59.6 (C), 99.2 (C), 120.7 (C), 128.9 (CH), 131.7 (CH), 144.6 (C), 149.1 (C), 152.3 (C), 165.6 (C). All data for **BA11-O** are in accordance with those reported elsewhere.[50]

Ethyl 4-(4-bromophenyl)-6-methyl-2-thioxo-1,2,3,4-tetrahydropyrimidine-5-carboxylate (**BA11-S**): 78% yield (purified by precipitation). IR (KBr, ν cm^{-1}): 3328, 3174, 2982, 1670, 1578, 1198, 1122, 596. M.p.: 192.0-194.4 °C (Lit. M.p.: 191-192 °C). [56] ^{1}H-NMR (200 MHz, DMSO-d_6) δ 1.09 (t, 3H, J = 7.0 Hz), 2.29 (s, 3H), 4.00 (q, 2H, J = 7.0 Hz), 5.15 (brs, 1H), 7.17 (d, 2H, J = 8.1 Hz), 7.55 (d, 2H, J = 8.1 Hz), 9.67 (s, 1H), 10.38 (s, 1H). ^{13}C-NMR (50 MHz, DMSO-d_6) δ 14.0 ($\underline{C}H_3$), 17.2 ($\underline{C}H_3$), 53.6 ($\underline{C}H_2$), 59.7 (CH), 100.2 (C), 120.8 (CH), 126,6 (CH) 131.5 (CH), 142.8 (C), 145.4 (C), 165.0 (C), 174.3 (C). All data for **BA11-S** are in accordance with those reported elsewhere.[56]

Ethyl 6-methyl-2-oxo-4-phenyl-1,2,3,4-tetrahydropyrimidine-5-carboxylate (**BA12-O**): 68% yield (purified by precipitation). IR (KBr, ν cm^{-1}): 3246, 3116, 2980, 1726, 1648, 1192. M.p.: 205.3-207.3 °C (Lit. M.p.: 202-203 °C).[52] ^{1}H-NMR (400 MHz, DMSO-d_6) δ 1.09 (t, 3H, J = 7.1 Hz), 2.25 (s, 3H), 3.98 (q, 2H, J = 7.1 Hz), 5.14 (d, 1H, J = 3.2 Hz), 7.23-7.25 (m, 3H), 7.30-7.34 (m, 2H), 7.73 (s, 1H), 9.19 (s, 1H). ^{13}C-NMR (100 MHz, DMSO-d_6) δ 14.0 ($\underline{C}H_3$), 17.8 ($\underline{C}H_3$), 54.0 (CH), 59.2 ($\underline{C}H_2$), 99.3 (C), 126.2 (CH) 127.3 (CH), 128.4 (CH), 144.0 (C), 148.3 (C), 152.2 (C), 165.4 (C). All data for **BA12-O** are in accordance with those reported elsewhere.[52]

Ethyl 6-methyl-4-phenyl-2-thioxo-1,2,3,4-tetrahydropyrimidine-5-carboxylate (**BA12-S**): 85% yield (purified by precipitation). IR (KBr, ν cm^{-1}): 3330, 3174, 3104, 1670, 1648, 1196, 1118. M.p.: 205.5-207.3 °C (Lit. M.p.: 208-209 °C).[55] ^{1}H-NMR (400 MHz, DMSO-d_6) δ 1.08 (t, 3H, J = 7.0 Hz), 2.29 (s, 3H), 4.01 (q, 2H, J = 7.0 Hz), 5.18 (d, 1H, J = 3.7 Hz), 7.21-7.36 (m, 5H), 9.63-9.64 (m, 1H), 10.32 (s, 1H). ^{13}C-NMR (100 MHz, DMSO-d_6) δ 26.9 ($\underline{C}H_3$), 30.0 ($\underline{C}H_2$), 66.9 ($\underline{C}H_3$), 72.4 ($\underline{C}H_2$), 113.6 (C), 139.3 (CH), 140.6 (CH), 141.4 (CH), 156.4 (C), 157.9 (C), 178.0 (C), 187.1 (C). All data for **BA12-S** are in accordance with those reported elsewhere.[55]

Ethyl 4-(4-hydroxybutyl)-6-methyl-2-oxo-1,2,3,4-tetrahydropyrimidine-5-carboxylate (**BA13-O**): 43% yield [purified by silica gel column chromatography using hexane/chloroform/ethyl acetate (3:3:4) as the eluant], IR (KBr, ν cm^{-1}): 3238, 3120, 2922, 1728,1704, 1646, 1096. M.p.: 234.7-238.6 °C (Lit. M.p.: 237-238 °C).[58] ^{1}H-NMR (200 MHz, DMSO-d_6) δ 0.82-1.37 (m, 10H), 1.57-1.67 (m, 4H), 2.16 (s, 3H), 3.92 (brs, 1H), 3.97-4.17 (m,2H), 7.30 (s, 1H), 8.89 (s, 1H). ^{13}C-NMR (50 MHz, DMSO-d_6) δ 14.2 ($\underline{C}H_3$), 17.7 ($\underline{C}H_3$), 25.7 ($\underline{C}H_2$), 25.9 ($\underline{C}H_2$), 26.0 ($\underline{C}H_2$), 26.3 ($\underline{C}H_2$), 28.5 ($\underline{C}H_2$), 44.9 (CH), 55.0 (CH), 59.0 ($\underline{C}H_2$), 98.0 (C), 148.4 (C), 153.2 (C), 165.8 (C). All data for **BA13-O** are in accordance with those reported elsewhere.[58]

Ethyl 4-cyclohexyl-6-methyl-2-thioxo-1,2,3,4-tetrahydropyrimidine-5-carboxylate (**BA13-S**): 4% yield [purified by silica gel column chromatography using hexane/ ethyl acetate (3:1) as the eluant]. IR (KBr, ν cm^{-1}): 3188, 2980, 2926, 1708, 1648, 1182, 1092. M.p.: 210.5-212.8 °C (Lit. M.p.: 207-208 °C).[59] ^{1}H-NMR (200 MHz, DMSO-d_6) δ0.78-0.90 (m, 1H), 1.07-1.22 (m, 7H), 1.37 (brs, 2H), 1.58-1.65 (m, 4H), 2.21 (s, 3H), 3.94-3.98 (m, 1H), 4.02-4.16 (m, 2H), 9.22-9.32 (m, 1H), 10.07 (s, 1H). ^{13}C-NMR (50 MHz, DMSO-d_6) δ 14.1 ($\underline{C}H_3$), 17.1 ($\underline{C}H_3$), 25.5 ($\underline{C}H_2$), 25.7 ($\underline{C}H_2$), 24.9 ($\underline{C}H_2$), 26.6 ($\underline{C}H_2$), 28.3 ($\underline{C}H_2$), 44.7 (CH), 55.3 (CH), 59.7 ($\underline{C}H_2$), 99.5 (C), 145.3 (C), 165.6 (C), 175.2 (C). All data for **BA13-S** are in accordance with those reported elsewhere.[59]

Urease activity assay

Representative Biginelli adducts bearing electron donating or withdrawing groups that were also soluble in ethanol were screened for their potential to inhibit type III urease from C. ensiformis (jack bean). The reaction media contained 20 mM phosphate buffer (pH 7.0), 1 mM ethylenediaminetetraacetic acid (EDTA), 10 mM urea, and 12.5 mU jack bean urease in the presence or absence of 500 μM Biginelli adducts. Reactions were incubated at 25 °C, and after 10 min, they were stopped by adding 0.5 volumes of 1% (m/v) phenol in 5 mg L^{-1} sodium nitroprusside (SNP) followed by the addition of 0.7 volumes of 0.5% (m/v) NaOH solution in 0.1% NaOCl. The mixtures were incubated at 50°C for 5 min, and the absorbance was measured at 630 nm to determine the amount of NH_4^+ formed.[60] Urease inhibition was determined in terms of the percent of NH_4^+ formed in **BA**-containing reactions in relation to the total urease activity in the inhibitor-free reactions. Three independent experiments were performed with four replicates each.

Interaction studies

Interaction studies by molecular fluorescence.

Stock solutions of *C. ensiformis* (jack bean) type III urease (Sigma-Aldrich) at 10 μM were prepared in 20 mM phosphate buffer with 1 mM EDTA (pH 7), while the Biginelli adducts **BA5-S** and **BA7-S** were dissolved in ethanol to yield 1.0 mM solutions that were further diluted in phosphate buffer to provide the corresponding working solutions. Molecular fluorescence titrations were performed using quartz cuvettes with a 10 mm optical path on a Shimadzu spectrofluorometer (model 5301PC, Japan) equipped with a xenon lamp (150 W). The urease (1.0 μM) fluorescence emission spectra in the absence or presence of compounds **BA5-S** and **BA7-S** (2.5 to 50 μM) were recorded from 260 to 450 nm employing an λ_{ex} of 280 nm at three temperatures (22, 30, 38ºC). The excitation and emission slits were 5 and 10 nm, respectively. To calculate the critical distance

at which the energy transfer occurs from the urease tryptophan residues (5 μM) to the **BA5-S** and **BA7-S** (both at 5 μM), Förster Resonance Energy Transfer (FRET) studies were performed. Tridimensional fluorescence experiments were performed using an excitation wavelength in the range from 220-350 nm and a fixed emission range from 260 to 450 nm. Synchronous fluorescence spectra for urease in the absence or presence of Biginelli adducts **BA5-S** and **BA7-S** were obtained by simultaneous variation of the excitation and emission monochromators. The difference in the excitation wavelength (Δλ) was fixed individually at Δλ = 15 nm (Tyr) and Δλ = 60 nm (Trp) to show solely the spectroscopic behaviour of the Tyr and Trp residues. The inhibitors *N*-(*n*-butyl) thiophosphoric triamide (NBPT), thiourea, and omeprazole were used at the fixed concentration of 25 μM in the competitive assay, while the hydroxyurea concentration was 38 μM.

Kinetics studies

Reactions were set exactly as described for the screening experiments except that the Biginelli adducts **BA5-S** and **BA7-S** were used individually at concentrations that inhibit urease in the range from 30 to 40% (0.1 to 0.3 mM) in the presence of increasing concentrations of urea (1-32 mM). Reactions were stopped and analyzed as described for the screening experiments. The Michaelis-Menten hyperbolas and Lineweaver-Burk plots were obtained using the software OriginPro 8 (Origin Lab, Northampton, MA), and K_i values were determined using the experimental values of K_M, V_{max}, $K_{M\ app}$, $V_{max\ app}$, α and α'.

Molecular Dynamics and Docking simulation

For the molecular modeling studies, the acetohydroxamic acid (HAE) and Biginelli adducts (**BA5-S**, **BA7-S** and **BA10-S**) were constructed using the Marvin software [61] and jack bean urease (*C. ensiformis*) was obtained from the Protein Data Bank website (PDB entry: 4H9M). In order to obtain this hydrolase in its native state, molecular dynamics (MD) simulations were performed prior to docking studies. Thus, OPLS solvation model [62] was added to the urease structure. The simulations were performed using the GROMACS® package [63]. Water molecules and hydrogenionic concentration (pH 7.0) were added at the atomic level, considering a triclinic box. Geometries of the urease were optimized with the steepest descent algorithms followed by the conjugate gradient minimization. Two previous stabilization steps were performed at 1000 ps with a time step of 2 fs using NVT and, then, sets of 300 K NPT isobaric and isothermal to relax the water molecules, and to stabilize the box density. Then, MD simulations were carried out at 300 K for 30 ns (1 fs time step). The Lennard-Jones and the real-space part of electrostatic interactions were cut-off at 1.0 nm. For long-range electrostatic interactions, the particle-mesh Ewald (PME) method was used with the reciprocal-space interactions evaluated on a 0.12 nm grid with cubic interpolation of order four. The P-LINCS algorithm was used to constrain all bond lengths. Isotropic pressure coupling was applied using the Berendsen algorithm at 1 bar with a time constant of 3.0 ps and compressibility of 4.5×10^{-5} ·bar^{-1}. The Parrinello-Rahman velocity rescale thermostat algorithm was applied independently for protein and water molecules at 300 K. Periodic boundary conditions were applied in all directions. Molecular graphics and analyses were performed with the UCSF Chimera package.[64] The MD analysis module of the UCSF Chimera® was used to obtain the most predominant conformation of the enzyme into the system. Root mean square deviation (RMSD) values were calculated using GROMACS®, and all RMSD charts were generated by using Xmgrace® software.[65] Finally, the Ramachandran plot was generated from the RAMPAGE online server [66].

After MD simulations, the most stable conformation of the jack bean urease was selected for molecular docking studies. The optimization of the HAE (a co-crystallized ligand at the active site from urease enzyme used for the re-docking experiment) and Biginelli adducts studied was performed with the classic method, using AMBER 99bsc0 force field and assigning partial charges AM1-BCC, automatically performed by the USCF Chimera® dock prep module. The UCSF Chimera® package was utilized to perform all molecular docking simulations. Water molecules and counterions previously added in MD simulations were removed from the resulting structure. All simulations were carried out considering the area of the active site from the jack bean urease. In order to validate the docking protocol, the molecular alignment of co-crystallized ligands was performed using PyMOL® version 2.3.1 software (https://pymol.org). In sense, the co-crystallized HAE ligand was extracted and aligned with the HAE binding mode obtained by molecular docking by using the urease enzyme after 50 ns dynamics simulations. Thus, the molecular alignment value (RMSD in Ångström) was obtained to support our virtual protocol and proceeds. Furthermore, it is assumed that a reliable virtual protocol involving DM simulations and molecular docking should provide atomic alignment values up to 2.0 Å [67].

Reference

1 J. B. Sumner, *J. Biol. Chem.*, 1926, **69**, 435-441.
2 K. Kappaun, A. R. Piovesan, C. R. Carlini and R. Ligabue-Braun, *J. Adv. Res.*, 2018, **13**, 3–17.
3 L. V. Modolo, A. X. de Souza, L. P. Horta, D. P. Araujo and Â. de Fátima, *J. Adv. Res.*, 2015, **6**, 35–44.
4 P. Kafarski and M. Talma, *J. Adv. Res.*, 2018, **13**, 101–112.
5 B. P. Callahan, Y. Yuan and R. Wolfenden, *J. Am. Chem. Soc.*, 2005, **127**, 10828–10829.
6 B. Krajewska, *J. Mol. Catal. B Enzym.*, 2009, **59**, 9–21.
7 L. V. Modolo, C. J. da-Silva, D. S. Brandão and I. S. Chaves, *J. Adv. Res.*, 2018, **13**, 29–37.
8 M. J. Maroney and S. Ciurli, *Chem. Rev.*, 2014, **114**, 4206–4228.
9 C. Follmer, *J. Clin. Pathol.*, 2010, **63**, 424–430.
10 D. Y. Graham and M. Miftahussurur, *J. Adv. Res.*, 2018, **13**, 51–57.
11 K. X. Ruthrof, E. Steel, S. Misra, J. McComb, G. O'Hara, G. E. St. J. Hardy and J. Howieson, *Sci. Total Environ.*, 2018, **625**, 1–7.
12 H. Cantarella, R. Otto, J. R. Soares and A. G. de B. Silva, *J. Adv. Res.*, 2018, **13**, 19–27.
13 F. Colpaert, F. Ledoux, V. R. Belzen, US 2019 / 0039962 A1, 2019, 1–6.

14 A. Hameed, M. Al-Rashida, M. Uroos, S. U. Qazi, S. Naz, M. Ishtiaq and K. M. Khan, *Expert Opin. Ther. Pat.*, 2019, **29**, 181–189.
15 D. Tzemi and J. Breen, *Ecol. Model.*, 2019, **394**, 18–26.
16 J. Bzura and R. Koncki, *Enzyme Microb. Technol.*, 2019, **123**, 1–7.
17 Y. F. Rego, M. P. Queiroz, T. O. Brito, P. G. Carvalho, V. T. de Queiroz, Â. de Fátima and F. Macedo Jr., *J. Adv. Res.*, 2018, **13**, 69–100.
18 Â. de Fátima, C. de P. Pereira, C. R. S. D. G. Olímpio, B. G. de F. Oliveira, L. L. Franco and P. H. C. da Silva, *J. Adv. Res.*, 2018, **13**, 113–126.
19 L.V. Modolo, A. de Fátima, M. Giovanni, D. L. da Silva, V. S. S. Morais, BR 102013017356-8 A2, 2016, 1–14.
20 U. Rashid, I. Batool, A. Wadood, A. Khan, Z. ul-Haq, M. I. Chaudhary and F. L. Ansari, *J. Mol. Graph. Model.*, 2013, **43**, 47–57.
21 F. Tamaddon and S. Ghazi, *Catal. Commun.*, 2015, **72**, 63–67.
22 E. Artola, S. Cruchaga, I. Ariz, J. F. Moran, M. Garnica, F. Houdusse, J. M. G. Mina, I. Irigoyen, B. Lasa and P. M. Aparicio-Tejo, *Plant. Growth. Regul.*, 2011, **63**, 73–79.
23 (a) P. Biginelli, *Gazz. Chim. Ital.*, 1981, **21**, 455–461. (b) P. Biginelli, *Gazz. Chim. Ital.*, 1891, **21**, 497–500. (c) P. Biginelli, *Berichte Dtsch. Chem. Ges.*, 1891, **24**, 1317–1319. (d) P. Biginelli, *Berichte Dtsch. Chem. Ges.*, 1891, **24**, 2962–2967. (e) P. Biginelli, *Gazz. Chim. Ital.*, 1893, **23**, 360–413.
24 L. Horta, Y. Mota, G. Barbosa, T. Braga, I. Marriel, Â. de Fátima and L. Modolo, *J. Braz. Chem. Soc.*, 2016, **27**, 1512-1519.
25 A. Khan, J. Hashim, N. Arshad, I. Khan, N. Siddiqui, A. Wadood, M. Ali, F. Arshad, K. M. Khan and M. I. Choudhary, *Bioorganic. Chem.*, 2016, **64**, 85–96.
26 C. O. Kappe, *J. Org. Chem.*, 1997, **62**, 7201–7204.
27 K. K. Pasunooti, H. Chai, C. N. Jensen, B. K. Gorityala, S. Wang and X.-W. Liu, *Tetrahedron Lett.*, 2011, **52**, 80–84.
28 J. Yu, F. Shi and L. Z. Gong, *Acc. Chem. Res.*, 2011, **44**, 1156–71.
29 Q. Wang and W. Pei, *J. Iran. Chem. Soc.*, 2010, **7**, 318–321.
30 L. M. Ramos, A. Y. P. L. Tobio, M. R. dos Santos, H. C. B. de Oliveira, A. F. Gomes, F. C. Gozzo, A. L. de Oliveira and B. A. D. Neto, *J. Org. Chem.*, 2012, **77**, 10184–10193.
31 M. Terada, K. Machioka and K. Sorimachi, *J. Am. Chem. Soc.*, 2007, **129**, 10336–10337.
32 D. J. Adams, P. J. Dyson and S. J. Tavener, *Chemistry in Alternative Reaction Media*, John Wiley & Sons, 2003, vol. 41, pp. 75–93.
33 S. Duan, X. Jing, D. Li and H. Jing, *J. Mol. Catal. Chem.*, 2016, **411**, 34–39.
34 Y. Jeong, D.-Y. Kim, Y. Choi and J.-S. Ryu, *Org. Biomol. Chem.*, 2011, **9**, 374–378.
35 T. O. Brito, A. X. Souza, Y. C. C. Mota, V. S. S. Morais, L. T. de Souza, Â. de Fátima, F. Macedo and L. V. Modolo, *RSC Adv.*, 2015, **5**, 44507–44515.
36 W. Yan-Qing and Z. Hong-Mei, *Spectrochim. Acta. A. Mol. Biomol. Spectrosc.*, 2012, **96**, 352–357.
37 A. Ghisaidoobe and S. Chung, *Int. J. Mol. Sci.*, 2014, **15**, 22518–22538.
38 H.-M. Zhang, G.-C. Zhang and Y.-Q. Wang, *Biol. Trace Elem. Res.*, 2011, **141**, 53–64.
39 T. Li, Z. Cheng, L. Cao and X. Jiang, *Food Chem.*, 2016, **194**, 740–748.
40 M. D. de A. Dantas, H. de A. Tenório, T. I. B. Lopes, H. J. V. Pereira, A. J. Marsaioli, I. M. Figueiredo and J. C. C. Santos, *Int. J. Biol. Macromol.*, 2017, **102**, 505–514.
41 T. C. A. Lage, T. M. S. Maciel, Y. C. C. Mota, F. Sisto, J. R. Sabino, J. C. C. Santos, I. M. Figueiredo, C. Masia, Â. de Fátima, S. A. Fernandes and L. V. Modolo, *New J. Chem.*, 2018, **42**, 5356–5366.
42 Y.-Q. Wang, G.-C. Zhang and H.-M. Zhang, *J. Solut. Chem.*, 2011, **40**, 458–469.
43 B. Valeur and M. N. Berberan-Santos, *Molecular fluorescence: principles and applications*, Wiley-VCH Verlag GmbH & Co. KGaA, Weinheim, 2001, pp.273-350.
44 C. C. Santana, E. F. Silva-Júnior, J. C. N. Santos, É. E. da S. Rodrigues, I. M. da Silva, J. X. Araújo-Júnior, T. G. do Nascimento, L. A. O. Barbosa, C. B. Dornelas, I. M. Figueiredo, J. C. C. Santos and L. A. M. Grillo, *Bioorganic. Chem.*, 2019, **87**, 169–180.
45 M. de M. Silva, T. S. Macedo, H. M. P. Teixeira, D. R. M. Moreira, M. B. P. Soares, A. L. da C. Pereira, V. de L. Serafim, F. J. B. Mendonça-Júnior, M. C. A. de Lima, R. O. de Moura, E. F. da Silva-Júnior, J. X. de Araújo-Júnior, M. D. A. Dantas, E. de O. O. Nascimento, T. M. S. Maciel, T. M. de Aquino, I. M. Figueiredo and J. C. C. Santos, *J. Photochem. Photobiol. B*, 2018, **189**, 165–175.
46 P. D. Ross and S. Subramanian, *Biochemistry*, 1981, **20**, 3096–3102.
47 F. Mehranfar, A. K. Bordbar, M. Keyhanfar and M. Behbahani, *J. Lumin.*, 2013, **143**, 687–692.
48 Y. Shu, W. Xue, X. Xu, Z. Jia, X. Yao, S. Liu and L. Liu, *Food Chem.*, 2015, **173**, 31–37.
49 J. C. N. Santos, I. M. da Silva, T. C. Braga, Â. de Fátima, I. M. Figueiredo and J. C. C. Santos, *Int. J. Biol. Macromol.*, 2018, **113**, 1032–1040.
50 Q. Wang, X. Liu, M. Su, Z. Shi and H. Sun, *Spectrochim. Acta. A. Mol. Biomol. Spectrosc.*, 2015, **136**, 321–326.
51 M. R. Siddiqui, Z. A. AlOthman and N. Rahman, *Arab. J. Chem.*, 2017, **10**, S1409–S1421.
52 A. Balasubramanian and K. Ponnuraj, *J. Mol. Biol.*, 2010, **400**, 274–283.
53 F. M. Oliveira, L. C. A. Barbosa, A. J. Demuner, C. R. A. Maltha, S. R. Pereira, L. P. Horta and L. V. Modolo, *Med. Chem. Res.*, 2014, **23**, 5174–5187.
54 Z. Amtul, B. S. P. Atta-ur-Rahman, R. Siddiqui and M. Choudhary, *Curr. Med. Chem.*, 2002, **9**, 1323–1348.
55 F. Iftikhar, Y. Ali, F. Ahmad Kiani, S. Fahad Hassan, T. Fatima, A. Khan, B. Niaz, A. Hassan, F. Latif Ansari and U. Rashid, *Bioorganic Chem.*, 2017, **74**, 53–65.
56 J.-Y. Cheng and Y.-H. Chu, *Tetrahedron Lett.*, 2006, **47**, 1575–1579.
57 F. M. A. Geilen, B. Engendahl, A. Harwardt, W. Marquardt, J. Klankermayer and W. Leitner, *Angew. Chem. Int. Ed.*, 2010, **49**, 5510–5514.
58 D. L. da Silva, F. S. Reis, D. R. Muniz, A. L. T. G. Ruiz, J. E. de Carvalho, A. A. Sabino, L. V. Modolo and Â. de Fátima, *Bioorg. Med. Chem.*, 2012, **20**, 2645–2650.
59 B. Zeynizadeh, K. A. Dilmaghani and M. Yari, *Phosphorus Sulfur Silicon Relat. Elem.*, 2009, **184**, 2465–2471.
60 D. L. da Silva, S. A. Fernandes, A. A. Sabino and Â. de Fátima, *Tetrahedron Lett.*, 2011, **52**, 6328–6330.
61 N. S. Nandurkar, M. J. Bhanushali, M. D. Bhor and B. M. Bhanage, *J. Mol. Catal. Chem.*, 2007, **271**, 14–17.
62 J. Zhu, M. Zhang, B. Liu and X. Li, *Chem. Lett.*, 2009, **38**, 56–57.
63 F. Shirini, K. Rad-Moghadam and S. Akbari-Dadamahaleh, *Green Solvents II: Properties and Applications of Ionic Liquids*, Springer Netherlands, Dordrecht, 2012, pp. 289–334.
64 A. Mobinikhaledi, M. Zendehdel, M. H. Nasab and M. A. B. Fard, *Heterocycl. Commun.*, 2009, **15**, 451-458.
65 P. Kumar, A. Kumar, S. S. Verma, N. Dwivedi, N. Singh, M. I. Siddiqi, R. P. Tripathi, A. Dube and N. Singh, *Exp. Parasitol.*, 2008, **120**, 73–79.
66 A. R. Gholap, K. Venkatesan, T. Daniel, R. J. Lahoti and K. V. Srinivasan, *Green Chem.*, 2004, **6**, 147–150.
67 K. S. Atwal, B. C. O'Reilly, J. Z. Gougoutas and M. F. Malley, *Heterocycles*, 1987, **26**, 1189–1192.
68 M. W. Weatherburn, *Anal. Chem.*, 1967, **39**, 971–974.

View Article Online
DOI: 10.1039/C9NJ03556G

69 M. F. Sanner, *J. Mol. Graph. Model.*, 1999, **17**, 57–61.
70 X. Jiang, W. Li, G. Chen and L. Wang, *J. Chem. Inf. Model.*, 2017, **57**, 288–297.
71 S. Pronk, S. Páll, R. Schulz, P. Larsson, P. Bjelkmar, R. Apostolov, M. R. Shirts, J. C. Smith, P. M. Kasson, D. van der Spoel, B. Hess and E. Lindahl, *Bioinformatics*, 2013, **29**, 845–854.
72 M. M. Silva, E. O. O. Nascimento, E. F. Silva, J. X. de Araújo, C. C. Santana, L. A. M. Grillo, R. S. de Oliveira, P. R.R.Costa, C. D. Buarque, J. C. C. Santos and I. M. Figueiredo, *Int. J. Biol. Macromol.*, 2017, **96**, 223–233.
73 P. J. Turner, *Xmgrace*, 2005.
74 S. C. Lovell, I. W. Davis, W. B. Arendall, P. I. W. de Bakker, J. M. Word, M. G. Prisant, J. S. Richardson and D. C. Richardson, *Proteins Struct. Funct. Bioinforma.*, 2003, **50**, 437–450.
75 E. F. Da Silva-Júnior, P. H. B. França, F. F. Ribeiro, F. J. B. Mendonça-Júnior, L. Scotti, M. T. Scotti, T. M. De Aquino and J. X. De Araújo-Júnior, *Curr. Comput. Aided Drug Des.*, 2018, **14**, 68–78.

GRAPHICAL ABSTRACT

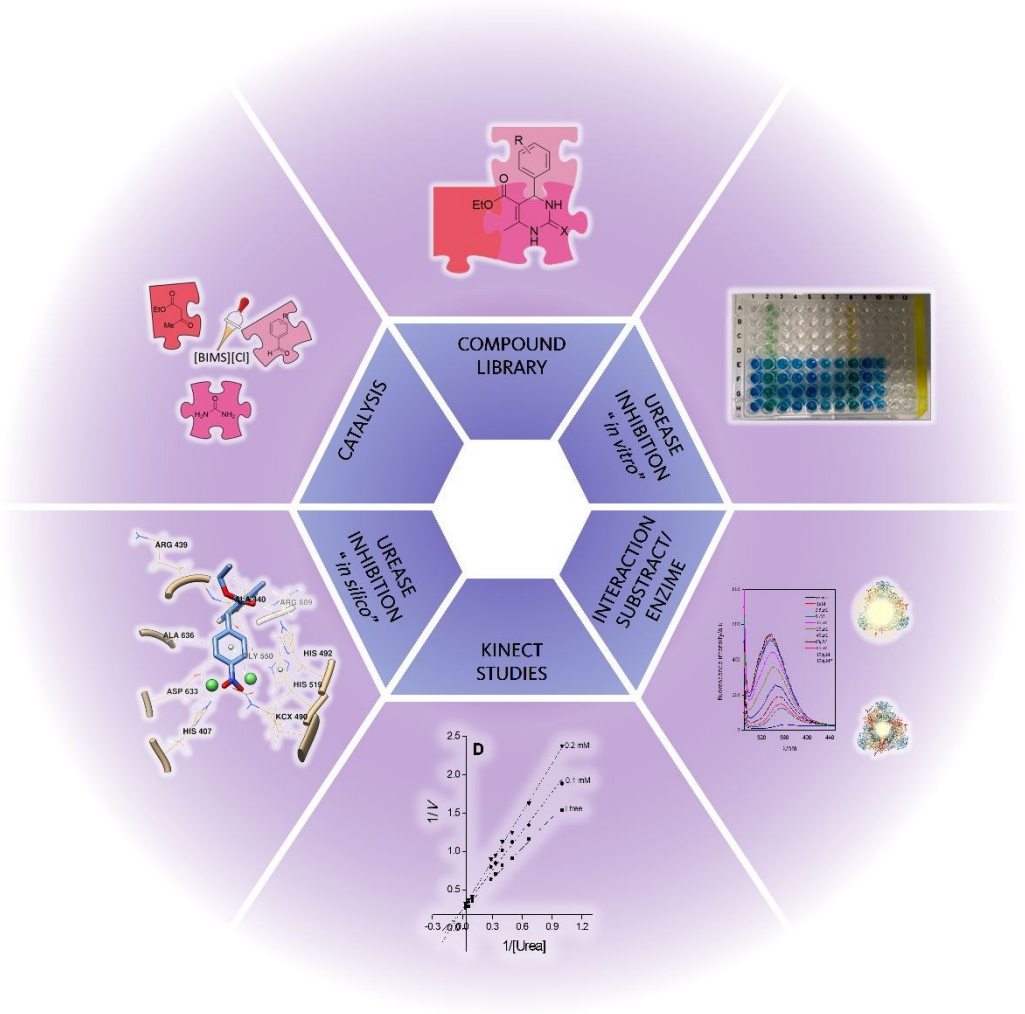

Three out of twenty-six synthesized Biginelli adducts were identified as potent competitive urease inhibitors.